ADVANCED SCIENCE
Open Access

WILEY-VCH

Dear Author,

Please correct your galley proofs carefully and return them no more than three days after the page proofs have been received.

If you have not used the PXE system before, please view the Tutorial before checking your proofs: http://wileypxe.aptaracorp.com/pxewileyvch/UserDocument/UserGuide/WileyPXE5_AuthorInstructions.pdf

Please note any queries that require your attention. These are indicated with red Qs in the pdf or highlighted as yellow queries in the "Edit" window.

Please pay particular close attention to the following, as no further corrections can be made once the article is published online:

- **Names** of all authors present and spelled correctly

- **Titles** of authors are correct (Prof. or Dr. only: please note, Prof. Dr. is not used in the journals)

- **Addresses of all authors** and **e-mail address of the corresponding author** are correct and up-to-date

- **Funding bodies** have been included and grant numbers are accurate

- The **Title** of the article is OK

- All **figures** are correctly included

- **Equations** are typeset correctly

Note that figure resolution in the PXE system is deliberately lower to reduce loading times. This will be optimized before the article is published online.

Please send any additional information, such as figures or other display items, to advancedscience@wiley.com, and please also indicate this clearly in the PXE "Edit" window by inserting a comment using the query tool.

Reprints may be ordered by filling out the accompanying form.
Return the reprint order form by e-mail with the corrected proofs, to Wiley- VCH: **advancedscience@wiley.com**

Please limit corrections to errors already in the text. Costs incurred for any further changes will be charged to the author, unless such changes have been agreed upon by the editor.
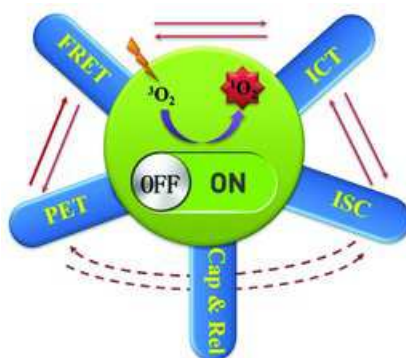
The editors reserve the right to publish your article without your corrections if the proofs do not arrive in time. Note that the author is liable for damages arising from incorrect statements, including misprints.

ADVANCED SCIENCE

Reprint Order Form 2017
- please return with your proofs -

Manuscript No. _____

Please send me and bill me for

[   ] no. of **reprints** via   ☐ airmail (+ 25 Euro)
                                     ☐ surface mail

☐ **high-resolution PDF file** (330 Euro).

My e-mail address:

_____

Please note: It is not permitted to present the PDF file
on the internet or on company homepages

★**Special Offer**★ If you order 200 or more reprints you
will get a PDF file for half price.

Information regarding VAT
Please note that from German sales tax point of view, the charge for
Reprints, Issues or Posters is considered as **"supply of goods"** and
therefore, in general, such delivery is a subject to German sales tax.
However,this regulation has no impact on customers located outside of the
European Union. Deliveries to customers outside the Community are
automatically tax-exempt. Deliveries within the Community to institutional
customers outside of Germany are exempted from the German tax (VAT)
only if the customer provides the supplier with his/her VAT number.
The VAT number (value added tax identification number) is a tax
registration number used in the countries of the European Union to identify
corporate entities doing business there. It starts with a country code (e.g.
FR for France, GB for Great Britain) and follows by numbers.

Cover Posters

Posters are available of all the published covers and
frontispieces in two sizes

[   ] DIN A2 42 x 60 cm/ 17 x 24in (one copy: **39 Euro**)

[   ] DIN A1 60 x 84 cm/ 24 x 33in (one copy: **49 Euro**)

Postage for shipping posters overseas by airmail:
+ 25 Euro

Postage for shipping posters within Europe by surface mail:
 + 15 Euro

Mail reprints / cover posters to:

_____
_____
_____
_____
_____
_____

Invoice address:

_____
_____
_____
_____
_____

_____
Date, Signature   **Stamp**

VAT no.: _____
(institutes / companies in EU countries only)

Purchase Order No.: _____

Credit Card Payment

VISA, MasterCard, AMERICAN EXPRESS
Please use the Credit Card Token Generator located at the
website below to create a token for secure payment. The token
will be used instead of your credit card number.

Credit Card Token Generator:
https://www.wiley-vch.de/editorial_production/index.php

Please transfer your token number to the space below.

Credit Card Token Number:

Price list for reprints (The prices include mailing and handling charges. All Wiley-VCH prices are exclusive of VAT)

No. of pages	Price (in Euro) for orders of					
	50 copies	100 copies	150 copies	200 copies	300 copies	500 copies
1-4	345	395	425	445	548	752
5-8	490	573	608	636	784	1077
9-12	640	739	786	824	1016	1396
13-16	780	900	958	1004	1237	1701
17-20	930	1070	1138	1196	1489	2022
for every additional 4 pages	147	169	175	188	231	315

★ **Special Offer** ★ If you order 200 or more reprints you will get a PDF file for half price.

WILEY-VCH

W. Wu, X. Shao, M. Wu,* J. Zhao*

.........x–xx

Controllable Photodynamic Therapy Implemented by Regulating Singlet Oxygen Efficiency

Recent research progress towards controllable photodynamic therapy implemented by regulating singlet oxygen production efficiency is discussed in this Review. It is focused on the discussion of various design strategies of controllable photosensitizers, from the mechanisms of activatable photosensitizers themselves to their response to the special tumor microenviroments.

REVIEW

Author Proof

ADVANCED SCIENCE
Open Access

Photodynamic Therapy

www.advancedscience.com

Controllable Photodynamic Therapy Implemented by Regulating Singlet Oxygen Efficiency

Wenting Wu, Xiaodong Shao, Mingbo Wu,* and Jianzhang Zhao*

With singlet oxygen ($^1O_2$) as the active agent, photodynamic therapy (PDT) is a promising technique for the treatment of various tumors and cancers. But it is hampered by the poor selectivity of most traditional photosensitizers (PS). In this review, we present a summary of controllable PDT implemented by regulating singlet oxygen efficiency. Herein, various controllable PDT strategies based on different initiating conditions (such as pH, light, H_2O_2 and so on) have been summarized and introduced. More importantly, the action mechanisms of controllable PDT strategies, such as photoinduced electron transfer (PET), fluorescence resonance energy transfer (FRET), intramolecular charge transfer (ICT) and some physical/chemical means (e.g. captivity and release), are described as a key point in the article. This review provide a general overview of designing novel PS or strategies for effective and controllable PDT.

1. Introduction

Photodynamic therapy (PDT) is a promising noninvasive approach for the treatment of cancer tumors by combining photosensitizer (PS), oxygen molecule and light.[1] In clinical applications, a low toxic or non-toxic PS is delivered to the tumor tissue and cancer cells by active or passive diffusion. Subsequently, PS is excited from its low energy ground state (S_0) to an higher energy excited state (S_1) by irradiating tumor tissue with long wavelength light (650–900 nm, light in this wavelength range gives good tissue penetration). In the treatment process, reactive oxygen species are responsible for destroying cancer cells, and the first singlet excited state of molecular oxygen (singlet oxygen, $^1O_2$) is the key cytotoxic agent of PDT.[2] $^1O_2$ is effective in disrupting biological tissues as a result of its high reactivity.[3] It is generated by the triplet-triplet energy transfer (TTET) between ground-state oxygen (triplet state) and PS (T_1) formed by intersystem crossing (ISC, **Figure 1**).[4]

ISC is an important non-radiation process in the photochemical and photophysical fields, which is also a pivotal mechanism for the generation of $^1O_2$.[5] Usually, ISC takes place between

Prof. W. Wu, X. Shao, Prof. M. Wu
State Key Laboratory of Heavy Oil Processing
China University of Petroleum
Qingdao, 266580, China
Prof. W. Wu, Prof. J. Zhao
State Key Laboratory of Fine Chemicals
School of Chemical Engineering
Dalian University of Technology
Dalian, 116024, P. R. China
Correspondence to: Prof. M. Wu (E-mail: wumb@upc.edu.cn), Prof. J. Zhao (E-mail: zhaojzh@dlut.edu.cn)
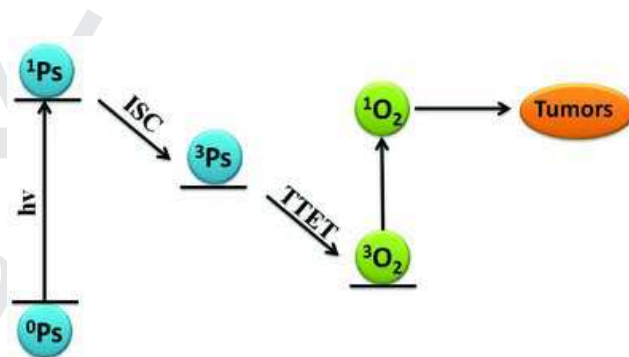
Figure 1. The generation of $^1O_2$ by intersystem crossing (ISC) and triplet-triplet energy transfer (TTET).

different energy levels such as S_1 to T_n or T_1 to S_0, and the quantum yield of ISC can be influenced by various factors such as heavy atom effect,[6] electron configuration,[7] perturbation of oxygen,[8] and so on. To the best of our knowledge, the generation of $^1O_2$ is mainly achieved by TTET, which takes from PS's triplet to ground oxygen (triplet state). Therefore it is possible to modulate the generation of $^1O_2$ by turning ISC efficiency with disparate environments.[9]

There is no doubt that PS is essential for valid PDT.[9b,10] Hence, research was focused on improving the properties of PS by designing novel sensitizers. The following requirements are essential for an ideal PS: (1) low cytotoxicity and high biocompatibility,[10a] (2) long-wavelength absorption,[11] (3) selective uptake into the cancer tissues and specific release $^1O_2$,[12] (4) effective ISC and a long-lived triplet excited state (high $^1O_2$ quantum yield).[13] However, most of traditional PS, with no selectivity and damage of normal cells, hardly meet the aforementioned criteria. Therefore, it is essential to design a novel

ADVANCED SCIENCE NEWS

www.advancedsciencenews.com

Author Proof

ADVANCED SCIENCE
Open Access

www.advancedscience.com

Q3
Q4
Figure 2. An illustration of all control mechanisms described in this review. Cap and Rel indicate factitious captivity and release mentioned in section 6.1.

PS which can be controlled as required, giving rise to $^1O_2$ on/off responses in cancer and normal cell, respectively.

Recently, controllable photosensitization process, in which $^1O_2$ are supposed to be modulated on demand, has received increasing attention.[14] Comparing with traditional PS, only in tumor region can $^1O_2$ be released and little normal cells are damaged. The formation of $^1O_2$ is prerequisite for an efficiently controllable photosensitization. As mentioned before, the generation of $^1O_2$ is directly related to ISC. Hence, the critical issue is how to regulate ISC efficiency. In fact, ISC is a kind of inactive pathway in the process of excited-state molecular deactivation, and there are many other mechanisms promoting the inactivation of excited-state molecules such as photoinduced electron transfer (PET),[15] fluorescence resonance energy transfer (FRET),[16] and intramolecular charge transfer (ICT).[17] Two or more inactive pathways are always competed with each other during the exciton deactivation. If ISC plays a dominant role, $^1O_2$ can be produced, that is $^1O_2$-ON state. Otherwise, production of $^1O_2$ is quenched or inhibited if other pathways suppress ISC, this is $^1O_2$-off state. In summary, it is a novel strategy to regulate $^1O_2$ quantum yield indirectly by modulating ISC efficiency. Of course, the physical captivity and controlled release of PS, such as delivery carriers based on the peptide and protein,[18] are also good ways to directly control PDT process.

Attention has been paid to efficient and selective control in the $^1O_2$ quantum yield. In this review, we focus on the modulation of production of $^1O_2$ based on various pathways developed since the year 2000. The categorizations of the articles are based on different mechanism of action. To better understand all control mechanisms mentioned in this work, a simple illustration and a summative comparisons table were given in **Figure 2** and **Table 1**. We hope to provide a general overview of designing novel PS or strategies for effective and controllable PDT.

Wenting Wu received her BS and PhD in fine chemical engineering from Dalian University of Technology in 2007 and 2012, respectively. She was a visiting scholar in 2014 at the OSAKA University, and is currently an associate professor at China university of petroleum. Her research interests include electron/energy transfer in photochemistry and photophysics, triplet-triplet annihilation upconversion, PDT, photocatalysis and so on.

Xiaodong Shao obtained his B. E. degree in chemical engineering from Shandong University of Technology in 2014. She is currently pursuing his M. S. degree in the chemical engineering, China University of Petroleum in china, under the supervision of Prof W. Wu and Prof. M. Wu. His current interest is focused on developing novel photosensitizers for photocatalysis and photodynamics therapy (PDT).

Professor Jianzhang Zhao received his PhD degree at Jilin University, China, in 2000. Then he carried out postdoctoral research at Pohang University of Science and Technology (South Korea), the Max Planck Research Unit for Enzymology of Protein Folding (Germany) and the University of Bath (UK) from 2000 to 2005. He took his current position in 2005. His research interest is focused on the development of new triplet photosensitizers, ranging from synthetic chemistry, study of the photochemical and photophysical properties with femto- and nanosecond transient absorption/emission spectroscopy, to computation chemistry.

Q5

2. PET Regulation Mechanism

PET[19] can be used to modulated the generation of $^1O_2$ when compete with others mechanisms, especially ISC. It is well known that $^1O_2$ quantum yield is directly related to the effi-

ADVANCED SCIENCE NEWS

www.advancedsciencenews.com

Author Proof

ADVANCED SCIENCE

Open Access

www.advancedscience.com

Table 1. Summative comparisons of all control mechanisms mentioned in this work.

Item	Control Requirements	Converted Means/Methods	Advantages	Disadvantages
Object				
PET	electron donor/acceptor	pH (acid), solvent polarity	highly effective, strong expansibility, programmable	need to specially design electron donor/acceptor, less conversion means
FRET (inhibitive/ reversible)	energy donor/acceptor, FRET-linker, spectral overlap, limited distance, energy level matching	pH (acid), enzyme, DNA, H_2O_2, light	versatile, readily, highly effective, programmable, strong expansibility	need to specially design energy donor/acceptor, complicated systems
ICT	electron donor/acceptor	pH (acid), solvent polarity	highly effective, programmable	need to specially design electron donor/acceptor less research
Factitious captivity and release of PS	governable and decomposable Frameworks	pH (acid)	simple mechanism, highly effective, strong expansibility, multifunction	multicomponent system, complex strategies, less conversion means
Chemical release and capture of $^1O_2$	activatable endoperoxides	temperature	intermittent PDT, bright future	no O_2 self-sufficient, less research

ciency of ISC (generally, high ISC efficiency results in high $^1O_2$ quantum yield). Usually, PET and ISC are competitive with each other in the process of deactivation of excited states. Therefore, given charge recombination won't lead to formation of triplet state, inhibition of PET can significantly improve the efficiency of ISC, resulting in an enhancement of $^1O_2$ quantum yield. Therefore, the generation of $^1O_2$ can be controlled by modulating PET process.

For the controllable PET system,[15b,20] it is always composed of electron donor (D) and acceptor (A), which can be separated from each other in solution.[21] Combining previous excellent works, it was shown that a PET process can be regulated by many stimulus, such as ions, pH, carbohydrates, phosphates, etc.[22]

O'Shea et al.[23] reported a strategy to modulate the generation of $^1O_2$ by PET mechanism with pH variation of the solution. $^1O_2$ quantum yield is controlled by switching on/off of the PET process. In order to achieve such a tuning effect, amine (as a specific receptor for H^+ and PET donor) was attached to PDT agents by covalent bond (**Figure 3**). In the absence of the substrate (that is H^+), the unbound receptor is with a rapid quench of the PS excited state by PET process, thereby $^1O_2$ production is shut down (Figure 3, pathway A). In contrast, $^1O_2$ generation would occur if acid was added, as the PET pathway would be switched off by the protonation of the amine (Figure 3, pathway B).

Tetsuo Nagano et al.[24] reported a novel strategy for controlling the generation of $^1O_2$. The environment-sensitive PSs (ESPers) could be active in hydrophobic (low-polarity) environment for high $^1O_2$ generation while little $^1O_2$ production was observed in polar cytosolic environment (**Figure 4**).[24] The ESPers are supposed to bind inositol 1,4,5-trisphosphate receptor which bears a strong-affinity hydrophobic moiety.[25,26] In decay of the excited PS, photosensitization and PET always compete with each other, resulting in the decrease of fluorescence or $^1O_2$. The PET process is known to depend on the highest occupied molecular orbital (HOMO) energy level of the electron donor and
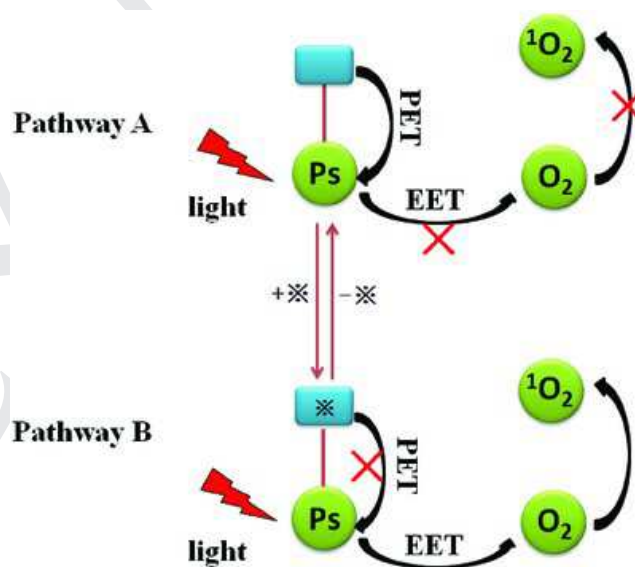

Figure 3. The modulation mechanism of $^1O_2$ based on PET. Substrate-specific receptor is shown in blue; PS is shown in green. Black cross () represents the substrate. Adapted with permission.[23] Copyright 2005, American Chemical Society.

the solvent polarity, so they designed and synthesized a series of PS derivatives attached with various electron donor moieties.

As shown in Figure 4, **2a-2f** were all 2I-BDP derivatives with different substituents (methyl, methoxy and amino) as PET donor for obtaining various HOMO energy level. The $^1O_2$ production of the compounds with high HOMO energy level can be effectively shut down by polar solvents. So the $^1O_2$ quantum yield of these 2I-BDP derivatives could indeed be modulated by PET. **1c–1e** could hardly generate $^1O_2$ in solvents more polar than acetone (dielectric constant, DC ≈ 20.7), while the photosensitization ability was restored in solvents less polar than CH_2Cl_2 (DC ≈ 9.14). It turned out that 2I-BDP derivatives with HOMO energy around −0.17 to −0.19 hartree could be taken as
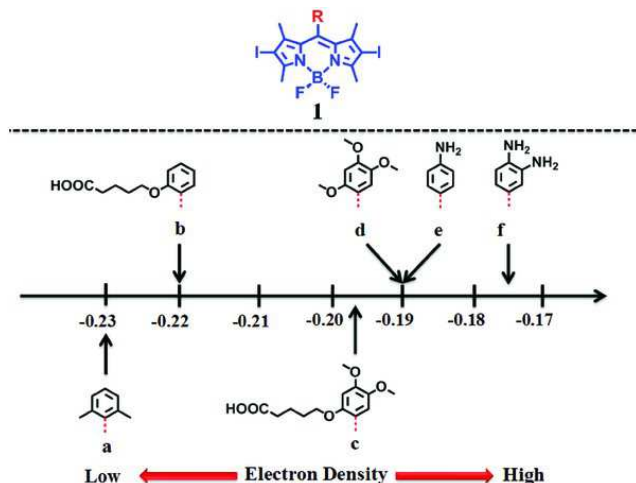
Figure 4. Chemical structures of 2I-BDP derivatives and electron density of various substituent. Reproduced with permission.[24] Copyright 2008, National Academy of Sciences
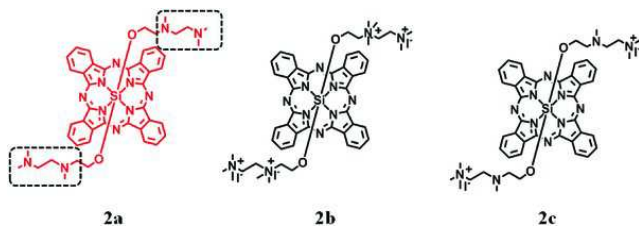

Figure 5. The structure of silicon-phthalocyanines PSs. Reproduced with permission.[22c] Copyright 2010, The Royal Society of Chemistry.

ESPers, which would be activated in a hydrophobic environment while little $^1O_2$ was generated in a polar environment.

Novel strategies which can modulate fluorescence emission and quantum yield of $^1O_2$ by pH-sensitive compounds have received considerable attentions.[22c] Phthalocyanine is an effective PS which can reveal significant acid-dependent $^1O_2$ generation by appropriate substitution.[27] Ng et al. proposed a pH-dependent $^1O_2$ photosensitization with silicon(IV) phthalocyanine as PS (**Figure 5**).[22c] Compound **2a** (B band at 352 nm, Q band at 684 nm in water) was prepared by mixing the silicon phthalocyanine dichloride with ethanol in the presence of pyridine in toluene. Compound **2b** (di-*N*-methylated derivative) and **2c** (tetra-*N*-methylated derivative) are considered as reference. The productivity of $^1O_2$ is enhanced by 3 times when the pH reduces from 7.4 to 6.0, as a result of protonation of the amino groups which can inhibit the PET process effectively.

Another way to modulate the quantum yield of $^1O_2$ by PET mechanism is to prepare an appropriate crown ether and pyridine substituted boron-dipyrromethene (BODIPY, **Figure 6**). Akkaya and co-workers[28] showed this BODIPY derivative could generate more $^1O_2$ when two different signals were present under the same conditions, that is a AND logical gate.[29] It is a remarkable fact that the pH of tumor tissues can be very low,[30] while intracellular sodium ion concentration is almost 3 times higher than in healthy ones.[31] So they combined crown ether with pyridyl–styryl substituents in BODIPY (**3a**) to ensure higher
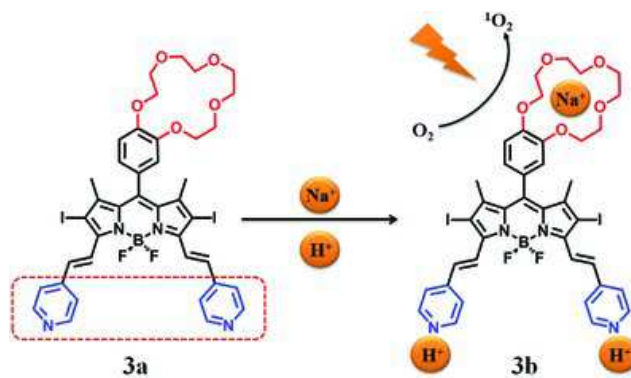
Figure 6. Chemical structure of BODIPY derivatives and the AND logical gate for PDT. Adapted with permission.[28] Copyright 2009, American Chemical Society.

sensitivity for both proton and sodium ion concentrations in tumor cells.

$^1O_2$ quantum yield are enhanced by 5 times when both Na$^+$ and H$^+$ are present. While an apparent low rate of output was observed when neither trifluoroacetic acid (TFA) nor Na$^+$ was present or only TFA was present. Herein, amino is the donor of PET and crown ether is acceptor. One interpretation for this phenomenon may be that PET channel is remarkably inhibited due to the presence of Na$^+$ and H$^+$, resulting in high efficiency ISC and restored $^1O_2$ generation. In contrast, there is still a strong PET process when only TFA or Na$^+$ is present. However, the experimental conditions (concentration and acid) is beyond the limits of biocompatibility normal standard. No further biological related researches were reported.

By synthesizing dimethylaminostyryl BODIPY-C$_{60}$ dyads and triads, Zhao et al. achieved pH-controllable modulation of $^1O_2$ based on PET.[32] The visible light-trapping antenna BODIPY moieties are regarded as PET-donor and singlet energy donor, while C$_{60}$ groups are considered as PET-acceptor and singlet energy acceptor (**Figure 7**).[32] 4a is dyads (λ_{abs} = 573 nm, λ_{em} = 591 nm) while **4b** is triads (λ_{abs} = 504/574 nm, λ_{em} = 587 nm). In the absence of acid, the S$_1$ state energy level of the dimethylaminostyryl-BODIPY moieties is higher than that of C$_{60}$, so there is an efficient energy transfer from BODIPY to C$_{60}$ (thus the S$_1$ state of C$_{60}$ is populated). However, the triplet excited state (T$_1$) would be quenched by efficient PET from BODIPY part to C$_{60}$. As a result, little $^1O_2$ is generated by TTET, and this is the $^1O_2$-off state. In the presence of acid, PET effect will be inhibited due to the protonation of dimethylamino, so the triplet excited state of BODIPY part cannot be quenched and $^1O_2$ would be produced by TTET, this is the $^1O_2$-ON state. For **4a**, the singlet oxygen quantum yield is 1.9% at neutral condition and 73% in acid. For **4b**, that is 2.0%/1.8% in neutral and 52%/63% in acid, respectively.

3. FRET Regulation Mechanism

FRET was used for the structural analysis of DNA,[33] protein,[34] targeted therapy,[35] fluorescent probe,[36] biosensors[37] etc.[38]

ADVANCED
SCIENCE NEWS

www.advancedsciencenews.com

Author Proof

ADVANCED
SCIENCE
Open Access

www.advancedscience.com
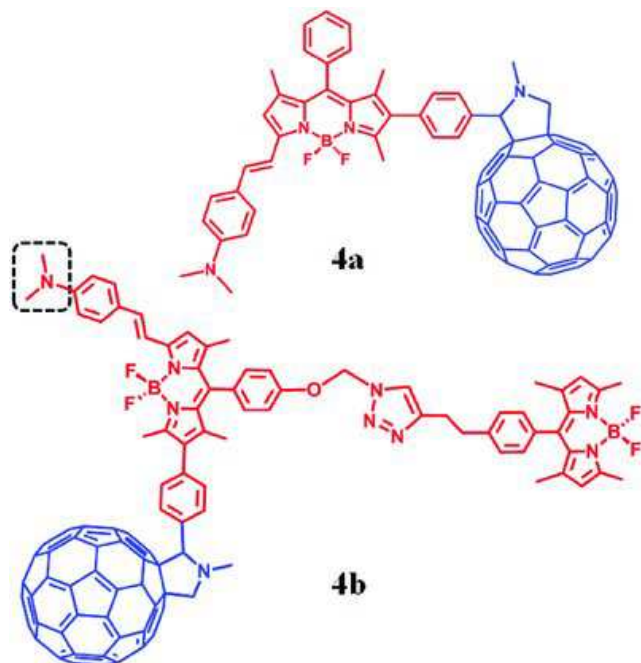
Figure 7. The structure of BODIPY-C$_{60}$ dyads (**4a**) and triads (**4b**).
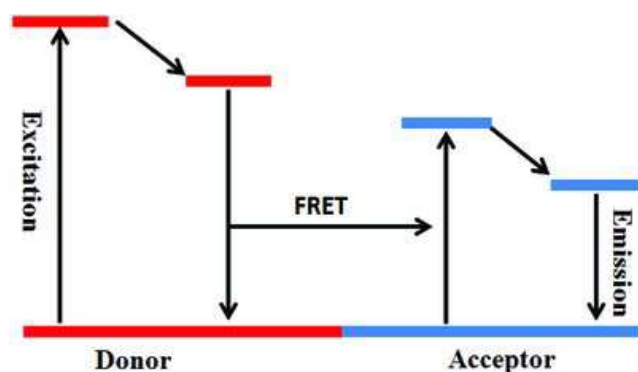

Figure 8. The mechanism of the FRET process.

When there is a spectral overlap between energy donor (D, emission spectrum) and energy acceptor (A, acceptor absorption), the fluorescence of the donor will be quenched, and the fluorescence of the energy acceptor will be observed (**Figure 8**).[39] FRET is achieved upon donor-acceptor energy transfer based on a long-range dipole–dipole interaction. Energy transfer includes two main mechanisms: (1) resonance energy transfer (RET) between the singlet state of donor and acceptor, namely Förster resonance energy transfer (FRET); (2) the other is RET between triplet state of the donor and singlet state of acceptor, that is Dexter electron transfer mechanism.[40] FRET occurs when: (1) there is a spectral overlap between D and A; (2) proper distance between D-A, normally less than 10 nm; (3) a relatively high quantum yield in donor.[41] The FRET fluorescence quenching always correlates with $^1O_2$ quenching, providing a convenient method to assess activatable photosensitizers.[42]
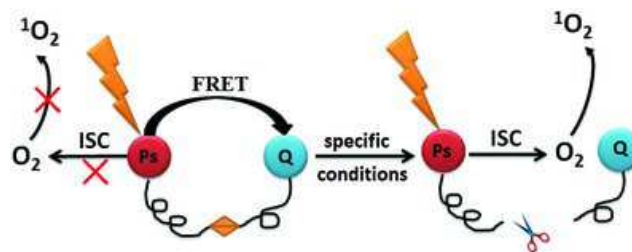
Figure 9. The modulation mechanism of $^1O_2$ based on FRET. Red ball, PS; Blue ball, quencher.

3.1. Inhibitive FRET

FRET is a kind of RET mechanism.[43] FRET can be used to regulate the generation of $^1O_2$ given it can compete with other excited state relaxation processes such as ISC, PET, etc. Therefore, in order to regulate $^1O_2$ quantum yield, it is necessary to promote or decrease FRET intensity, to drain the singlet excited state of the energy donor (which is responsible for ISC and thus production of the singlet oxygen). As mentioned before, FRET can be influenced by the distance between the donor and acceptor.[44] In order to control FRET, donor and acceptor are often combined via a special linker which can be sensitive to various specific triggers, such as some special enzymes related to tumors. Energy transfer between D and A can be terminated once the linker is cleaved by reacting with specific substrates.

Based on these mechanisms, some novel compounds combining with PSs, cleavable linker and $^1O_2$ quencher were designed as photodynamic molecular beacons (PMB).[45] Herein, PS is the donor of the FRET, and the quencher is the energy acceptor (**Figure 9**). In this case, an efficient energy transfer between PS and acceptor will inhibit the singlet oxygen production. Little or no $^1O_2$ will be generated unless the linker is cleaved by some specific conditions in tumors, namely, photosensitization is in off state in normal cells. In tumor cells, the linker will be cleaved in the presence of the specific conditions (pH value and specific enzymes); therefore PS and the quencher are separated with each other and energy transfer (FRET) will be forbidden, resulting in the restoration of the photosensitization, and $^1O_2$ can be generated via irradiation.

An controllable PMB with caspase-cleavable peptide as the linker was prepared by Zheng et al.,[46] in which chlorophyll analog pyropheophorbide (absorption at 667 nm, $^1O_2$ quantum yield >50%)[47] was used as the PS moiety (D) while carotenoid (A) was the quencher of $^1O_2$ and triplet excited states energy acceptor (**Figure 10**).[46] As mentioned above, when conveyed into target-area, the PMB was cleaved in the presence of caspase, and the carotenoid and pyropheophorbide is no longer linked by a covalent bond, thus results in the production of $^1O_2$; in contrast, little $^1O_2$ can be produced in normal cells due to an effective energy transfer between pyropheophorbide and carotenoid.

In previous studies, caspase was regard as a molecular scissor to cleave the specific peptide sequence, results in inhibition of FRET. Nevertheless, it is hard to evaluate the PDT in apoptotic cells with this agent, because caspase itself is a cell apoptosis marker. Hence, it is essential to find new enzyme and specific cleavable peptide linker for effective FRET modulation. Accord-

ADVANCED SCIENCE NEWS

www.advancedsciencenews.com

Author Proof

ADVANCED SCIENCE
Open Access

www.advancedscience.com

Figure 10. The structure of caspase-controllable PMB. Red: pyropheophorbide (PS); Green: carotenoid (Q); Blue: caspase-cleavable linker. Adapted with permission.[46] Copyright 2009, American Chemical Society.
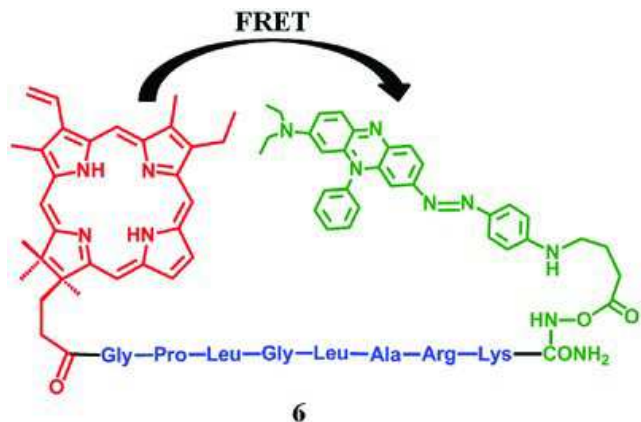

Figure 11. The structure of metalloproteinases-cleavable PMB. Red: pyropheophorbide (PS); Blue: peptide sequence (linker); Green: black hole quencher-3 (BHQ3, Q). Adapted with permission.[48] Copyright 2007, National Academy of Sciences

Figure 12. The structure of fibroblast-cleavable PMB. Adapted with permission.[49] Copyright 2009, American Chemical Society.

Figure 13. a) Structure of PS and quencher. b) the controlling mechanism of $^1O_2$ by DNA –controllable agent. Adapted with permission.[51] Copyright 2006, American Chemical Society.

ingly Zheng et al.[48] prepared a metalloproteinases-cleavable PMB. Matrix metalloproteinases are a family of extracellular proteinases and closely related to cancer and tumor progression. Notably, a short peptide sequence, GPLGLARK, was employed as a specificity-linker whose break can be induced by italics (**Figure 11**). It turned out that the MMP7-specific-peptide linker can be cleaved in MMP7-positive cells and the PS can be activated, resulting in 18-fold increase in $^1O_2$ quantum yield. Similarly, another PMB with fibroblast-cleavable linkers was synthesized by Zheng et al. in 2009 (**Figure 12**).[49] Herein, fibroblast activation protein is an initiator highly expressed in cancer-related fibroblasts of human epithelial carcinomas but not in normal fibroblasts or tissues.[50] Experiments show that peptide sequence linker could be cleaved effectively by fibroblast activation protein.

Gothelf et al.[51] reported a DNA sequence-specific PDT reagent based on reverse hybridization (**Figure 13**). Pyropheophorbide (PS, **8a**, absorption at 415 nm and fluorescence at 670 nm, $^1O_2$ quantum yield $= 0.53 \pm 0.04$) attached to a short 15-mer nucleotide sequence is the PS and BHQ3 (Q, **8b**) attached to a 21-mer oligonucleotide is the quencher (Figure 13a).[51] By DNA-programmed assembly, PS and Q are in proximity,[52] resulting in an effective FRET effect which can restrain the $^1O_2$ generation. When another DNA sequence is introduced into this system, P-DNA linker could be replaced and released, resulting in a recovery of photosensitization, then $^1O_2$ can be produced with irradiation (Figure 13b).[51]

Guo et al.[53] report a novel multifunction nanoparticles which can achieve targeted transport, controllable PDT and effective supply of O_2, simultaneously. Herein, poly(D,L-lactic-co-glycolic acid) (PLGA) was used as the framework of the multifunction nanoparticles; methylene blue (MB) (PS) and catalase were placed in the aqueous core, and BHQ3 doped into the PLGA shell was chosen as an quencher of PDT effect. In addition, cyclic pentapeptide incorporated on the surface of nanoparticle was regarded as the targeting ligand. (**Figure 14**).[53] There is an efficient FRET between MB and catalase which can restrain the in vitro generation of $^1O_2$. The nanoparticles could be absorbed in vivo by tumors selectively. Subsequently, H_2O_2 enters into the core of nanoparticles, O_2 would be produced by the catalytic action of catalase, resulting in the crack of PLGA and release of
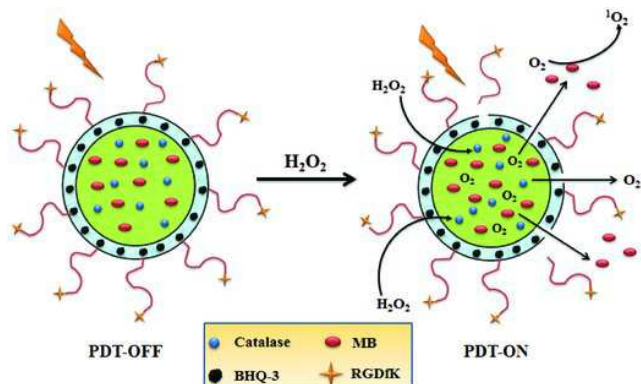
ADVANCED SCIENCE NEWS

www.advancedsciencenews.com

Author Proof

ADVANCED SCIENCE
Open Access

www.advancedscience.com

Figure 14. The structure of H_2O_2-activatable multifunction nanoparticles and its working principles. Adapted with permission.[53] Copyright 2015, American Chemical Society.
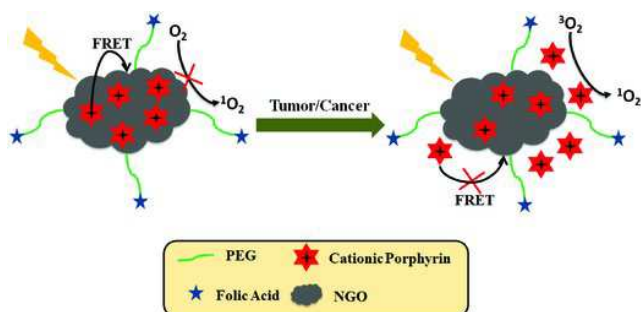

Figure 15. The structural representation of dual-targeting (cellular targeting and subcellular targeting) nanosystem and its regulation mechanism. Adapted with permission.[57] Copyright 2015, American Chemical Society.

MB. Photosensitization is recovered and $^1O_2$ is generated with the termination of FRET. Notably, the strategy could give a targeted and efficient PDT with controllable PDT and autarkic O$_2$.

Compared with the normal physiological pH, the tumor or cancer cell are with weakly acidic feature. This acidic environment could also be used to control the FRET process in PDT. It has been demonstrated that nanographene oxide (NGO) could be regarded as carrier to convey PS[54] and build tumor-targeted[55] or photothermal treatment system.[56] Interestingly, NGO would be preferable to separate from the PS in acid condition. Thus, Wu et al. designed a dual-targeting (cellular targeting and subcellular targeting) nanosystem to control PDT.[57] In this nanosystem, a cationic porphyrin was used as $^1O_2$ PS, which is loaded onto the surface of the polyethylene glycol (PEG)-functionalized and folic acid-modified nanographene oxide (NGO-based carrier for MitoTPP) through electrostatic interaction and π-π stacking (**Figure 15**). PEG chains could enhance NGO's water dispersibility and biocompatibility; the folic acid moiety can specifically target the folate receptor-positive cells. Under light irradiation, NGO can effectively inhibit the $^1O_2$ generation until MitoTPP is released from its carrier in acidic environment (tumor cells).

Instead of effect on the linker, the low pH could also influence the PS. In this case, the PSs are usually designed with amino groups (the H^+ proton acceptor in acid condition).[58] For example, combining dimethylaminostyryl BODIPY with C$_{60}$, Zhao
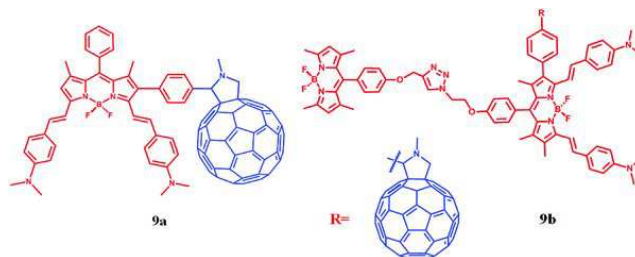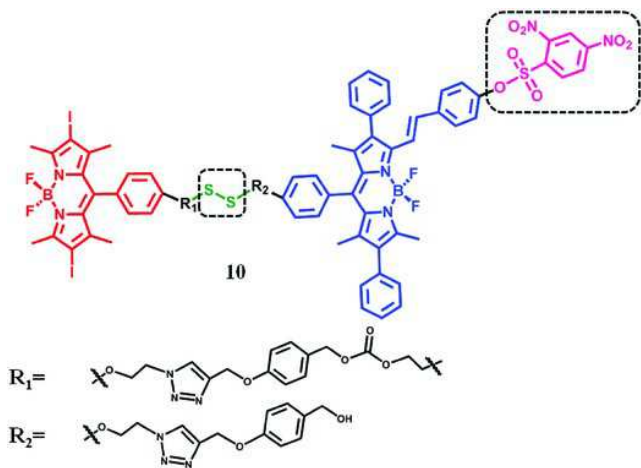

Figure 16. The structure of dimethylaminostyryl BODIPY-C60 dyads and triads.

et al. proposed a method to switch the triplet excited states and $^1O_2$ quantum yield based on FRET.[32] The BODIPY moieties and C$_{60}$ part are attached with each other by Prato reaction. **9a** is dyads ($\lambda_{abs} = 627$ nm, $\lambda_{em} = 644$ nm) while **9b** is triads ($\lambda_{abs} = 502/627$ nm, $\lambda_{em} = 637$ nm, **Figure 16**).[32] In this case, BODIPY moieties are FRET-donor and light-harvesting antenna, while C$_{60}$ groups are FRET-acceptor. The S$_1$ state energy level of the BODIPY moieties in **9a** and **9b** are lower than C$_{60}$, resulting in an inhibited FRET from BODIPY to C$_{60}$. In addition, there is a lower charge transfer state which can quench triplet excited states. So little $^1O_2$ could be generated in this condition. When dissolved in acid, the S$_1$ state energy level of the BODIPY moieties would surpass the corresponding energy level of C$_{60}$ due to the protonation of dimethylaminostyryl. At the same time, the energy level of charge transfer state is enhanced. So the triplet excited states and $^1O_2$ could be produced. For **9a**, the $^1O_2$ quantum yield is 1.1% in neutral condition and 26% in acid. For **9b**, that is 1.0%/1.4% in neutral and 22%/17% in acid, respectively.

By integrating PDT with fluorescence imaging functionality in one molecule, theranostic is becoming a promising technology for the treatment of cancer.[59] Zhao et al.[60] reported a thiol-activated difunctional-PDT reagent **10** (**Figure 17**) for theranostic purpose, in which the PDT effect and fluorescence imaging are implemented by different moieties, giving rise to both high $^1O_2$ quantum yield and high fluorescence yield, simultaneously. The difunctional reagents are composed of PS, fluorophore (PL) and a disulfide bond (−S−S−), which can be cleaved by thiols such as Cys and GSH (Figure 17).[61] The iodine-BODIPY acts as PS and FRET-donor, while BODIPY serves as fluorescence unit and the FRET-acceptor. In the absence of thiols, the generation of $^1O_2$ can be quenched by FRET from iodine-BODIPY to BODIPY and the fluorescence of BODIPY can be inhibited by the 2,4-dinitrobenzenesulfonate moieties (DNBS). That is the off state of $^1O_2$ production and fluorescence. In the presence of thiols, FRET can be inhibited due to the cleavage of disulfide bond. So the efficiency of ISC is enhanced and the $^1O_2$ can be produced with the irradiation of PS. Simultaneously, the red fluorescence of BODIPY was observed as a result of the decomposition of the DNBS group by the thiols. It turned out that the $^1O_2$ quantum yield can be increased from 16.7%–71.5% and the fluorescence quantum yield can be enhanced from 1.3%–47.6%.

Besides the disulfide cleavage, some cancer-specific intracellular enzymes could also cut off the FRET process. Na et al. prepared core−shell nano PS consisting of polydopamine nanoparticle (PDNP) cores, surrounded by cancer-specific PS-conjugated hyaluronic acid (PS-HA) shells (**Figure 18**).[62] PS-HA play as the

ADVANCED SCIENCE NEWS

www.advancedsciencenews.com

Author Proof

ADVANCED SCIENCE
Open Access

www.advancedscience.com

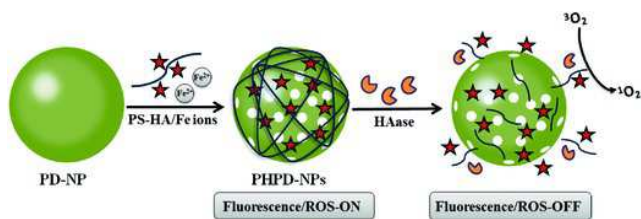**Figure 17.** The structure of thiol-activatable Bodipy–iodoBodipy dyads.

Figure 18. Synthetic routes of PS—hyaluronic acid conjugates shielded polydopamine nanoparticles (PHPD-NPs) and its $^1O_2$ on—off conversion. Adapted with permission.[62] Copyright 2016, American Chemical Society.
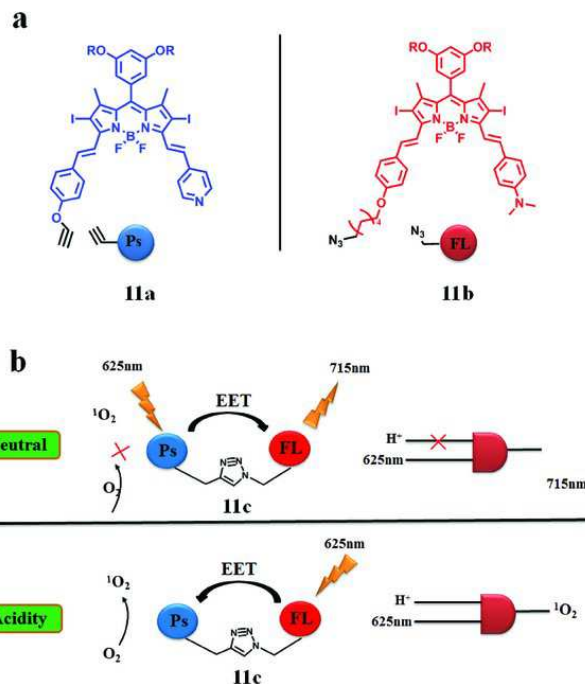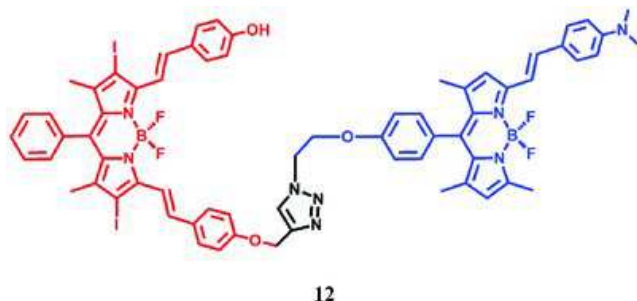

Figure 19. a) The chemical structure of PS and PL; b) working principle of DEMUX based on reversible FRET. Adapted with permission.[63] Copyright 2013, The Royal Society of Chemistry.

targeting moiety, while PDNP could quench the $^1O_2$ generation though FRET. The cancer-specific intracellular enzymes (e.g., hyaluronidase) is abundant in the tumor environment and plays key role for tumor proliferation and metastasis. This enzymes could separate the PS-HA shell from PDNPs and recover the $^1O_2$ generation ability of PS.

In fact, the key issues of controlling FRET effect are energy level matching and suitable linkers between the energy donor and the energy acceptor. As mentioned above, the overlapping extent of donor emission and acceptor absorption, namely their energy level matching, should be considered. Then, an appropriate linker should meet the following requirements: (1) bring the quencher and PS in close proximity, (2) being able to be selectively cleaved by specific factor (e.g. enzymes, pH). FRET-modulation takes advantage of specificity-linker to control the distance between donor and acceptor, resulting RET in on-off switching effect. In the deactivation of excited PS, FRET and ISC compete with each other. If FRET surpass ISC, a low $^1O_2$ quantum yield will be resulted; in contrast, once ISC is dominant, PS can be activated to produce $^1O_2$.

3.2. Reversible FRET

In an interesting example, the generation of $^1O_2$ can also be controlled upon the alterable direction of FRET. In this case, PS and FL are attached with each other, and there is an efficient

excited energy transfer (EET) between PS and FL. Under certain conditions, excited energy transfers from PS to FL occurs, leading to the quench of PS, namely, no or little $^1O_2$ is generated. However, under different condition, EET direction may be reversed, resulting in energy transfer from FL to PS, resulting in the activation of PS, therefore a high $^1O_2$ quantum yield is detected.

Based on this mechanism, a very innovative experiment has been reported by Akkaya.[63] A new strategy to control the on/off switching of $^1O_2$ production by a molecular 1:2 demultiplexer (DEMUX)[64] with FRET as the main mechanism. Actually, DE-MUX is a kind of chemical logic gate[65] and molecular logic gate,[66] which can generate various output signals with one input in demand. These switches are controllable. Therefore, if reactive oxygen species and fluorescence were output signals, demultiplexer can be used to combine diagnosis and therapy into one unity for PDT. Following this logic, Akkaya et al. designed compound **11c** (**Figure 19**) which was composed of two distyryl-Bodipy modules connected together by Huisgen cycloaddition. One part of compound **11c** is a PS (**11a**) with two iodine atoms to enhance the ISC efficiency; another one is a PL (**11b**) with a sensitivity to proton (Figure 19).

When excited at 625 nm in a neutral environment, compound **11c** gives an intense emission band at 715 nm, which is an output of DEMUX. In this case, EET takes place from the PS to FL. While in acid addition, upon excited at 625 nm, EET direction reverse which takes place from FL to PS, resulting in the generation of $^1O_2$ (Figure 19b). Actually, EET between PS and FL was a kind of FRET in this research. Generation of $^1O_2$ was switch off/on with the acid driven of the EET direction. There

ADVANCED SCIENCE NEWS

www.advancedsciencenews.com

Author Proof

ADVANCED SCIENCE
Open Access

www.advancedscience.com

Q11 **Figure 20.** The structure of the IodoBodipy-styrylBodipy dyads.

Figure 21. Common schematic representation of photocontrol $^1O_2$ on-off state. **Q12**

is a promising application for compound **11c**: when transferred into a given region such as tumor cells, compound **11c** can efficiently generate $^1O_2$ with fixed light irradiation for PDT, in the meantime, tumor cells and surrounding healthy tissues can be distinguished by different fluorescent intensity (healthy tissues are more brighter than tumor cells). No further biological researches were reported.

Zhao et al.[67] also reported an interesting iodoBodipy-styrylBodipy dyads **12** (**Figure 20**) which can be used to switch on/off the generation of $^1O_2$ based by the reversible FRET. The PDT-dyads are composed of the dimethylaminostyryl Bodipy moieties and the 4-hydroxylphenyl Bodipy part (Figure 20). In order to enhance the ISC efficiency, iodine atoms were introduced into Bodipy; at the same time, the introduction of dimethylaminostyryl is to ensure the sensitivity of PDT-dyads for acid. In the neutral condition, there is an effective FRET effect from hydroxylstyryl Bodipy group to dimethylaminostyryl Bodipy moieties, which can quench the fluorescence of the hydroxylstyryl Bodipy. In addition, the T_1 of the hydroxyl styryl Bodipy part could be quenched by the excited energy transfer between hydroxyl styryl Bodipy group and dimethylaminostyryl Bodipy moieties. In this case, little $^1O_2$ can be observed in this case ($\Phi_\Delta = 0.06$). In the presence of acid, the S_1 and T_1 state energy level of the dimethylamino styryl Bodipy group would be elevated, resulting in an inverse FRET effect from dimethylaminostyryl Bodipy moieties to hydroxylstyryl Bodipy group. Moreover, the formation of the charge transfer state is inhibited with the protonation of the dimethylamino group. So a long-lived T_1 state ($\tau_T = 1.6$ μs) and high-efficiency $^1O_2$ quantum yield ($\Phi_\Delta = 0.59$) were observed for **12**. In should be noted that the photophysical properties of this dyads can be recovered completely with the acid neutralized by base.

Notably, the critical factor in regulating FRET is how to change the donor and acceptor energy level by external stimulus. As mentioned above, various chemical stimuli (such as pH, enzyme) have been employed to modulate the properties of PS, resulting in on/off or high/low $^1O_2$ quantum yield. In these systems, however, there are still some drawbacks limiting their application in PDT, for instance: (1) some control conditions is beyond the normal physiological conditions,[68] (2) control strategy such as enzymatic-cleavable FRET linkers or pH-manipulative PET are irreversible, namely, they cannot recover its original state. Herein, it is imperative to design new strategy for regulating $^1O_2$ on-off reversibly. Concerning this aspect, some compounds such as diarylethene derivatives can

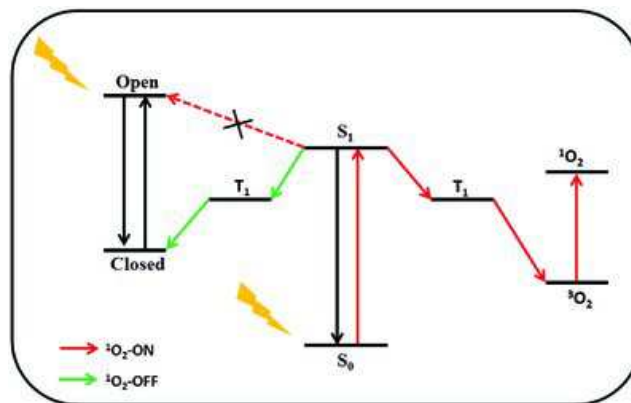interconvert between the open forms (with high energy levels) and closed forms (with low energy levels) upon irradiation at different wavelength,[69] which enable reversible FRET process. Thus, excited state of PS can be quenched by the energy transfer from PS to the closed forms of diarylethene, thus the production of $^1O_2$ is inhibited. Conversely, $^1O_2$ can be easily generated when the energy transfer between PS and the open forms of diarylethene is inhibitory (**Figure 21**).

Feringa et al.[70] designed a novel bicomponent system to modulate the generation of $^1O_2$ with photoirradiation as control (**Figure 22**). The bicomponent system are made up of diarylethene (photochromic switch, **13a**) and Zinc−tetraphenylporphyrin (PS, **13b**, $\Phi_\Delta = 0.84$).[71] When irradiated at UV and visible light, diarylethene molecular can interconvert between their colorless open and colored closed forms, respectively.[72] The molecular geometry and triplet energy levels of the open and closed forms of diarylethene are different. When diarylethene transforms into closed form with irradiation at 314 nm, triplet state energy transfer from **13b** (excited by 420 nm) to the closed form of the diarylethene suppresses the $^1O_2$ production; in contrast, the open form of diarylethene is dominant when irradiated by visible light (>470 nm). In this case, no triplet state energy transfer occurs and the $^1O_2$ can be generated effectively. The whole process of modulation is reversible. Later, this FRET mechanism was developed into supramolecular assemblies and MOF.

Liu et al. apply this reversible energy transfer mechanism into photo controlled supramolecular assemblies (**Figure 23**).[73] Dithienylethene-modified permethylated β-cyclodextrins and porphyrin derivatives forms assemblies in water through strong binding. Porphyrin is energy-donor and dithienylethene acts as energy-acceptor. Compared with other porphyrin/dithienylethene systems, this supramolecular assemblies system is with good water solubility and biocompatibility due to the introduction of permethyl-β-cyclodextrin. In addition, there is a high FRET efficiency (93.4%) between porphyrin and dithienylethene groups. The response of switch on/off for $^1O_2$ generation is fast (switch on-off: 50 s; switch off-on: 120 s).

Instead of supramolecular assemble system, Zhou et al. firstly developed this reversible FRET mechanism into MOF
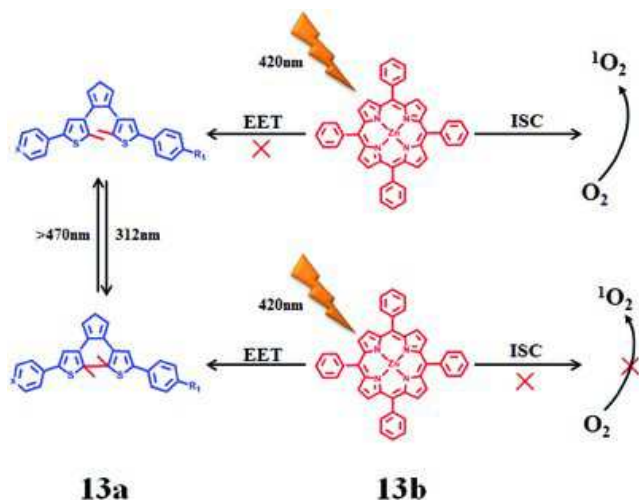
ADVANCED
SCIENCE NEWS
www.advancedsciencenews.com

Author Proof

ADVANCED
SCIENCE
Open Access

www.advancedscience.com

Figure 22. Controllable generation of $^1O_2$ based on photochemical switches of diarylethene. PS is shown in red and diarylethene is shown in blue. Adapted with permission.[70] Copyright 2014, American Chemical Society.
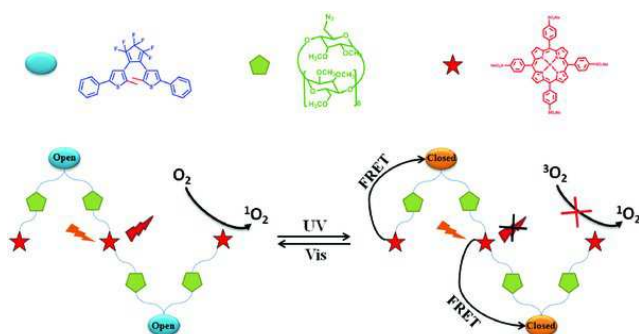

Figure 23. Schematic representation for photo-controlling $^1O_2$ on-off based on FRET conversion. Adapted with permission.[73] Copyright 2016, The Royal Society of Chemistry.

Figure 24. Defective UiO-66 with inserted porphyrin and diarylethene and their photoregulation $^1O_2$ generation process.

Figure 25. The structure of BODIPY dimer. Both M_1 and M_2 are BODIPY monomer. Reproduced with permission.[80] Copyright 2013, American Chemical Society.

system for the photooxidation of 1,5-dihydroxynaphthalene.[74] Then, they build another photosensitizing MOF system with UiO-66, porphyrin PSs and dithienylethene derivatives (fluorescent molecular switch) (**Figure 24**).[75] UiO-66 was regarded as a nanoplatform to storage and transport PDT agents. More importantly, it is possible to optimize the controllability of PDT performance by carefully modulating the ratios between PS and dithienylethene switch. In addition, without linkers between them, FRET happened efficiently in this MOF microenvironment, it successfully realize a reversible switch on/off of $^1O_2$ generation for PDT.

4. ICT Regulation Mechanism

ICT has been widely applied in many fields such as fluorescence probe,[76] fluorescent chemosensor,[77] etc.[78] By modulating the properties of the electron donor and acceptor, it is possible to change the efficiency of ICT. ICT can intensely impact the flu-
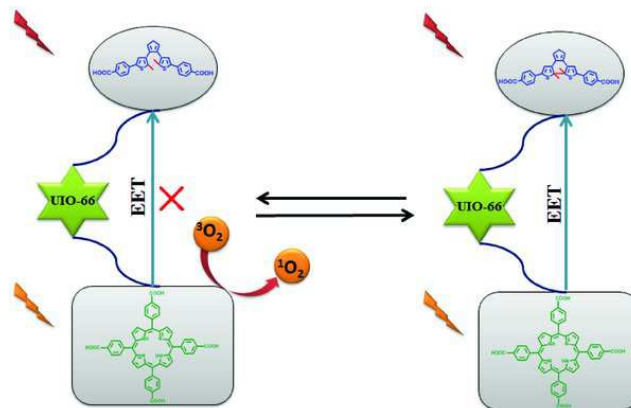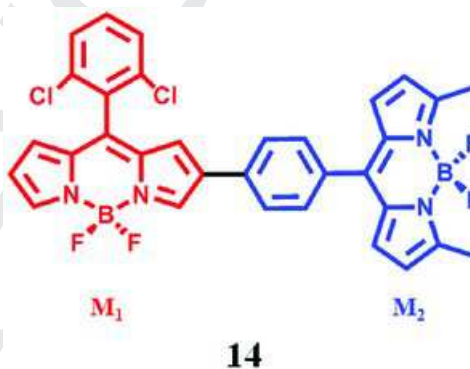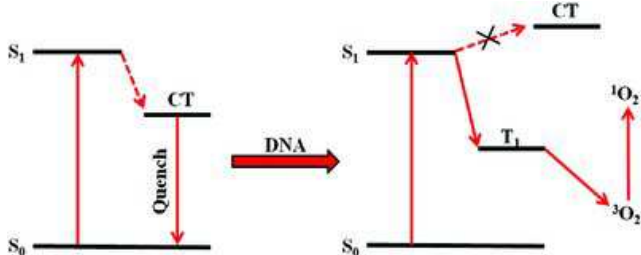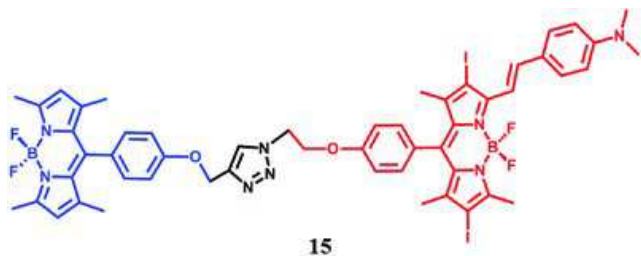
orescence and $^1O_2$ quantum yields via competing with other deactivation processes such as ISC and PET. There are many studies of the effect of the different donor and acceptor on ICT efficiency,[79] but little was known about the modulation of $^1O_2$ generation with ICT variation.

Yang et al.[80] prepared a BODIPY dimer (**14**) and investigated its mechanism of $^1O_2$ generation (**Figure 25**). It is interesting that the $^1O_2$ producing ability of this BODIPY dimer can change in non-polar/polar microenvironments. Only in low polar solvent (such as hexane, cyclohexane and toluene) can $^1O_2$ be generated significantly while no or little $^1O_2$ can be produced in polar solvent. Triplet excited state ($\tau_T = 49$ µs in argon-saturated hexane) only exists in BODIPY dimer rather than in BODIPY monomer, which is demonstrated by transient absorption spectra.[81] In fact, there is a significant ICT effect in polar solvents which can compete with ISC, resulting in quenching of the $^1O_2$ production.

Hirakawa et al. designed meso-(9-anthryl) tris(N-methyl-p-pyridinio) porphyrin, which is composed of anthracene (D) and porphyrin (A).[82] In this PS, the intramolecular electron transfer from the anthracene moiety to the porphyrin moiety forms a CT state, providing a fast deactivation pathway instead of producing $^1O_2$. Unlike previous pH modulation, the anionic DNA were used to interact with cationic porphyrin, and it inhibits

ADVANCED SCIENCE NEWS
www.advancedsciencenews.com

Author Proof

ADVANCED SCIENCE
Open Access
www.advancedscience.com

Figure 26. Schematic representation for DNA regulated $^1O_2$ generation based on ICT energy-level variation.

Q14

Figure 27. The structure of the dimethylaminostyryl iodoBodipy-Bodipy dyads.

Q15

Figure 28. a) Operational mechanism for the AND logic gates. Top: modulation of $^1O_2$; bottom: fluorescence self-reporting. b) The structure of Gate1 and Gate2. In Gate2, the donor of EET are shown in red part while blue part represents EET acceptor. Adapted with permission.[84]

the electron transfer quenching via rising the CT state energy level (**Figure 26**). The $^1O_2$ quantum yield increased to 0.22, no $^1O_2$ production was detected in the absence of DNA. Thus, the electron-donor connecting TMPyP type PS could control the photosensitized $^1O_2$ generation through this ICT mechanism.

Actually, ICT can compete with other processes as well, such as PET. Zhao et al.[67] proposed a strategy to modulate the $^1O_2$ generation by mainly controlling the ICT effect of PS. In this dyads, the dimethylaminostyryl iodo-Bodipy and the unsubstituted Bodipy are connected with each other (**Figure 27**). In the absence of acid, there is an effective FRET effect from unsubstituted Bodipy to dimethylaminostyryl iodo-Bodipy. However, the S_1 and T_1 of iodo-Bodipy can be quenched by the ICT effect, resulting in a low quantum yield of $^1O_2$ ($\Phi_\Delta = 0.07$). With the addition of acid, the ICT effect disappeared with the protonation of dimethylaminostyryl group, resulting in a long-lived dimethylaminostyryl ($\tau_T = 3.1$ µs) and a high $^1O_2$ quantum yield ($\Phi_\Delta = 0.74$). Again, the photophysical properties of this dyads can be recovered completely after the addition of base.

5. The Competition between EET and PET

In the generation of $^1O_2$, there are always several different mechanisms competing with each other, e.g. FRET, PET and ICT. They are mainly from the competition between energy transfer (EET) and electron transfer (PET). Derived from these competition, the emergence of molecular logic gates, emerged to finely tune the $^1O_2$ generation. Molecular logic gates, as a promising strategy,[83] was rarely applied to PDT. Combining molecular logic gates with PDT, Akkaya et al.[84] reported a controllable and self-reporting PDT, realized by series logic gate. The cascading of molecular logic gates are composed of two AND logic oper-
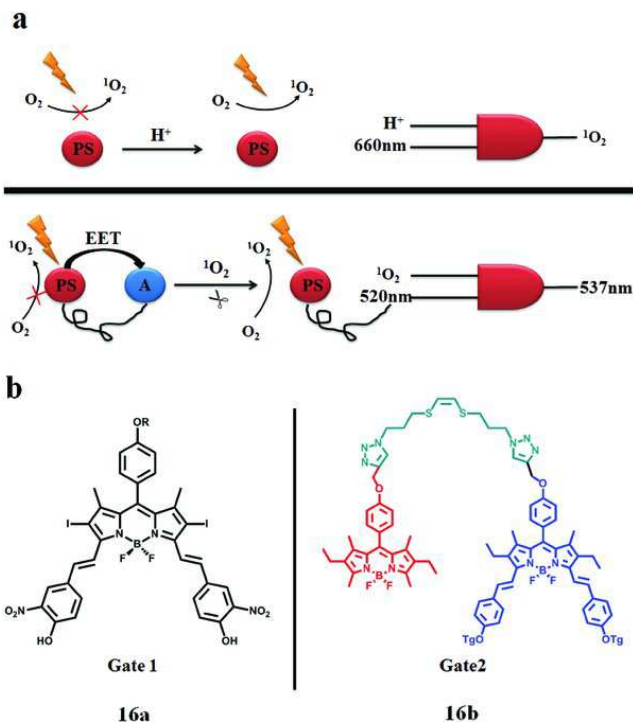
ation (**Figure 28**). In the first logic gates, light (660 nm) and acidic environment are input signal, $^1O_2$ is the output. BODIPY connected with two nitro ($pK_a = 6.92$) is responsible for Gate 1. Only in the presence of acid can $^1O_2$ be generated as a result of the protonation of Gate 1. There is no related interpretation mechanism for pH-controllable PDT. For the second logic gates, $^1O_2$ (the output of gate1) and 520 nm light are the input, the output is 537 nm light. Gate 2 is composed of an EET donor (D) and acceptor (A) portion which are connected to each other by a $^1O_2$-cleavable linker ((Z)-1,2-bis(alkylthio) ethane). In the absence of $^1O_2$, there is an effective excitation energy transfer (85.0%) between D and A, shutting down the production of $^1O_2$. In contrast, D can emit at 537 nm in the present of $^1O_2$ which can break the linker. Gates 1 and 2 were embedded together into a micelle for a continuous logic operation. When this logic gates are introduced into body, controllable-PDT efficiency can be revealed by the fluorescence intensity at 537 nm.

6. Factitious Captivity and Release

6.1. Factitious Captivity and Release of PSs

Besides regulating the PSs themselves via PET, FRET or ICT, there is another direct regulation method — captivity and release of PS or singlet oxygen. In this part, the $^1O_2$ PS is usually confined in the cage of core or shell part (e.g. nanoparticles, micelle or self-assembly), which are sensitive to the special envi-
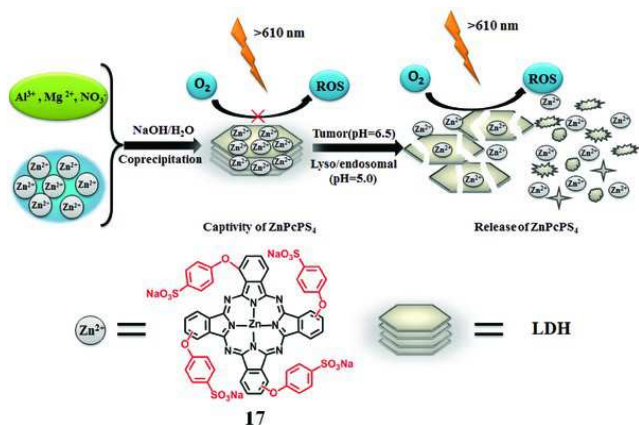
ADVANCED
SCIENCE NEWS

www.advancedsciencenews.com

Author Proof

ADVANCED
SCIENCE
Open Access

www.advancedscience.com

Figure 29. The synthetic route of LDH–ZnPcPS₄ and its working principle for controllable PDT. Adapted with permission.[85]
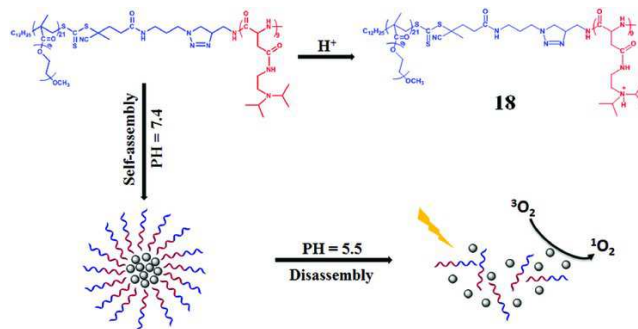

Figure 30. Structure of multifunctional polypeptide micelle and its pH-responsive PDT process. Adapted with permission.[58] Copyright 2016, American Chemical Society.
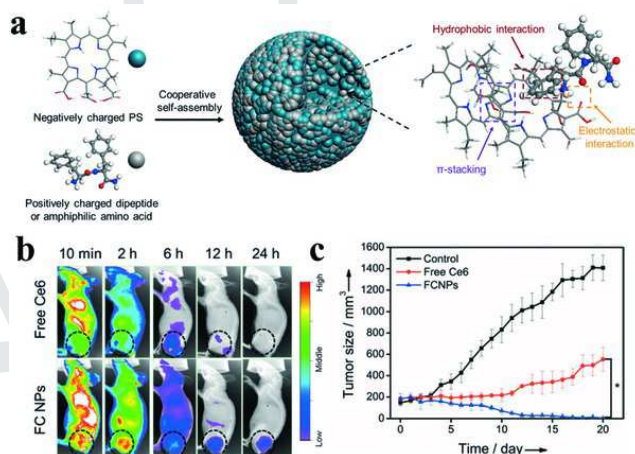

Figure 31. a) synthetic route of photosensitive nanoparticles based on amphiphilic dipeptide-tuned self-assembly. b) The fluorescence images of MCF7-tumor-bearing nude mice through a tail intravenous injection with FCNPs and free Ce6 (equivalent Ce6 4.0 mg kg⁻¹ body) at different times. tumor sites were shown in black circles. c) tumor growth test within 20 days. Reproduced with permission.[87]

ronment of cancer cell or tumor (e.g. low pH, high concentration of GSH). When the modified PSs comes to the special tumor environment, the active PSs could be released from the cage and generate ¹O₂. Some typical stimulated examples are listed below.

Huang et al.[85] provided an interesting and provident investigation about switching on/off the generation of ¹O₂ by a layered double hydroxide (LDH) with the pH-responsive property. Herein, zinc (II) phthalocyanine substituted with 4-sulfonatophenoxy groups (ZnPcPS4) combined with LDH via electrostatic interaction was synthesized (**Figure 29**).[85] When there is no acid, LDH–ZnPcPS4 has little capacity to generate ¹O₂ due to the stable structure of nanohybrid. However, in slightly acidic media (pH = 6.5 or 5.0), ZnPcPS4 can be efficiently released from the LDH carrier due to the collapse of the LDH structure, resulting in recovery of the photoactivities.

Liu et al. reported a pH-responsive multifunctional polypeptide micelle for simultaneous imaging and in vitro PDT (**Figure 30**).[58] The BODIPY-Br₂ was used for the efficient ¹O₂ generation. By hydrophobic interaction, BODIPY-Br₂ connected with amphiphilic copolypeptide micelles via a ring-opening polymerization and click reaction. It is worth to mention that the diisopropylethylamine groups conjugate to the polypeptide side chains. Under normal microenvironment, it forms the hydrophobic core of BODIPY-Br₂ and hydrophilic shell for improving the solubility and stabilization. However, at lower pH such as 5.5, the diisopropylethylamine groups could be protonated, and its role converts from the hydrophobicity to hydrophilicity. Subsequently, the core–shell structured micelle degrade and it could release BODIPY-Br₂ as shown in Figure 30.

Based on the peptide- and protein-Based assembly, Yan et al. develop a new type of delivery carriers for regulating photosensitization and enhancing PDT effects.[86] Compared with the free PSs, these assembly show enhanced PDT effect after the PSs released from these assembly. For example, 9-Fluorenylmethoxycarbonyl-1-lysine (an amphiphilic amino acid with antiinflammatory activity) and Chlorin e6 (Ce6, a model hydrophobic photosensitive drug) formed the self-assembly (FC-NPs) through electrostatic force, π-π stacking and hydrophobic interactions (**Figure 31**a).[87] These self-assembly could be stim-

ulated by pH, surfactant and enzyme as they are on-demand to release drug in tumors. The fluorescence intensity of Ce6 could reflect the the distribution and the concentration of FCNPs. The in vivo biodistribution showed that FCNP has a selective accumulation in the tumor (Figure 31b). Compared wtih free Ce6, the PCNPs exhibit sustained Ce6 fluorescence at the tumor site for 24 h. Due to this retention of photosensitive drugs in the tumor tissue, the tumors of FCNP-treated mice were suppressd and almost completely eradicated during the PDT (Figure 31c).

Instead of the most PS in the core part, Guo et al. confined the pH sensitive PS, 5-aminolevulinic acid Zn(II) coordination polymer (ALA-Zn^II) in the shell part, and magnetite colloidal supraparticles (Fe₃O₄) in the core part (**Figure 32**).[88] ALA could selectively accumulate in tumorous tissues and be metalized to the PS PpIX for producing ¹O₂ after the visible light irradiation. In this PS (Fe₃O₄@ALA-Zn^II), the ALA release could be triggered by a small pH variation (pH 7.4 to 6.0 and 5.0). Compared with ALA, Fe₃O₄@ALA-Zn^II has better PDT activity for
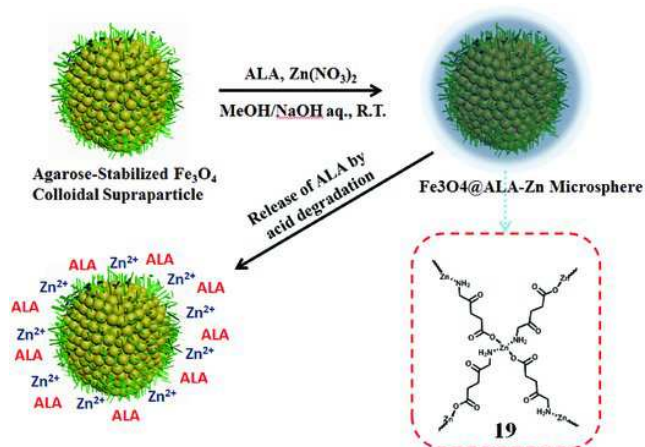
**ADVANCED
SCIENCE NEWS**

www.advancedsciencenews.com

Author Proof

**ADVANCED
SCIENCE**
Open Access

www.advancedscience.com

Figure 32. Preparation process of Fe_3O_4@ALA-ZnII microsphere and the pH-sensitive release of PS. Adapted with permission.[88]
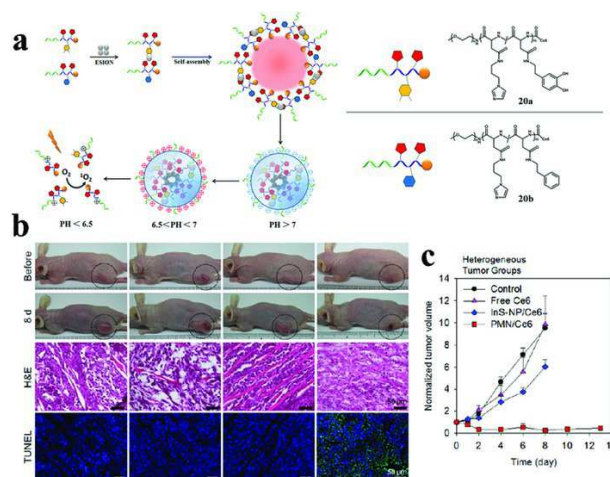

Figure 33. a) Synthetic route of pH-responsive Magnetic Nanogrenades and their photoactivity change in different pH levels. b) Upper: photograph of mice bearing heterogeneous tumors before and after PDT. Below: H&E and TUNEL staining of tumor tissue sections (c) Measured heterogeneous tumor volumes in the four treatment groups for 10 days. Reproduced with permission.[89] Copyright 2014, American Chemical Society.

T24 cells, and show good biocompatibility with the normal 293T cells.

The microenvironment of tumors is usually with a pH of ca. 6.8, and endo/lysosomes has even pH values of 5.0–5.5. Without any targeting agents, Hyeon et al.[89] reported the tumor pH-sensitive magnetic nanogrenades (PMNs, **Figure 33**), which is composed of self-assembled iron oxide nanoparticles (the core part for T_1 MRI contrast agent) and pH-responsive ligands (the shell part by incorporating ionizable moieties on the polymeric ligand). In this shell part, it involves a two-stage pH activation: (1) for increased cell adsorption and permeation at the tumor microenvironment, imidazole (pKa, ≈6.8) incorporated could impart pH sensitivity; (2) for releasing the diagnosis and PDT agents under tumor endo/lysosomal pH of ≈5.5, 3-phenyl-1-propylamine incorporated could produce a critical phase transition of PMNs, and destroy the self-assembly structure. The therapeutic effect of PMNs in tumors of more heterogeneous and drug-resistant nature were further demonstrated. Compared with pH-Insensitive Nanoparticle Assemblies (InS-NPs) and free Ce6, PMNs produced great tumor growth inhibition (Figure 33b, c). In the PMN treated group, many cells in the tumor tissue and microvasculature as well as fibroblasts showed considerable destruction. Therefore, this pH sensitivity plays an important role in the improved anticancer therapeutic efficacy of PMNs.

6.2. Chemical Control for $^1O_2$ Release and Capture

Instead of the above mentioned methods of capture and release of the PSs, $^1O_2$ could also be reversibly restored by chemical method in some cases. $^1O_2$ could reversibly react with some specific polycyclic aromatic hydrocarbons (e.g. naphthalene, anthracene or pyridine derivatives),[90] and form endoperoxide which can subsequent release $^1O_2$ via warming and revert to the original state. However, tumor hypoxia[91] and PDT-induced hypoxia[92] hinder the development of PDT. Intermittent irradiation is supposed for recovery of intracellular oxygen. To some extent, this chemical controlled $^1O_2$ strategy are supposed to relieve the deficiency of oxygen problem in PDT.

Anthracene is a good substrate to form stable endoperoxides at ambient temperature (or 37 °C), but these endoperoxides could rapidly and completely come to cycloreversion after heating. Based on this method, Yoon and Akkaya et al. make good use of plasmonic heating of gold nanorods for remote-control $^1O_2$ release.[93] In this PS, the anthracene derivative was firstly oxidized into endoperoxides (**Figure 34**) by the MB under irradiation in the presence of oxygen. Then amine-PEG-thiol coupling with endoperoxides used to increase water solubility and to target at the gold nanorods for the convenient thermal transport. When this PS irradiated with a laser with 830 nm at room temperature, the absorption intensity of singlet-oxygen trap (1,3-diphenylbenzofuran) at 414 nm decrease, indicating the generation of the singlet oxygen.

Later, Akkaya et al.[94] prepared a bifunctional PS composed of 2,6-dibromo distyryl BODIPY and 2-pyridone (**Figure 35**). 2,6-dibromo distyryl BODIPY is a high-efficiency PS with long-wavelength absorption; the endoperoxides of 2-pyridone and derivatives were reported to generate $^1O_2$ efficiently by clean (no side reactions) cycloreversion reactions. The circulating principle of this system is described as follows: when irradiated at 650 nm, compound **22a** is excited to produce $^1O_2$ by photosensitive process and a part of $^1O_2$ is stored in endoperoxide of 2-pyridone (**22b**); in contrast, $^1O_2$ can be released with the thermal cycloreversion of compound **22b** in the absence of light, compound **22a** is recovered at the same time. Obviously, this process is reversible.

There are also other methods appeared. For example, Lovell and his co-workers prepared a binuclear ruthenium(II) dimer (**Figure 36**) which is bridged by an alkene linker.[95] As the alkene linker is cleaved by MB with red-laser irradiation, there is an intermediate chemical amplification effect on the $^1O_2$ generation after the subsequent blue-laser irradiation. It is different from

ADVANCED SCIENCE NEWS

www.advancedsciencenews.com

Author Proof

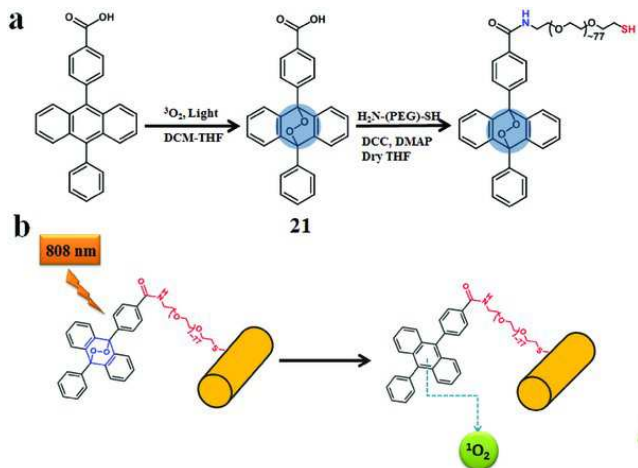**ADVANCED SCIENCE**
Open Access

www.advancedscience.com

Figure 34. a) Synthetic route of anthracene endoperoxide derivative and its further functionalization with gold nanorod; b) the release of singlet oxygen due to thermal cycloreversion of the endoperoxides upon plasmonic heating gold nanorods. Adapted with permission.[93]
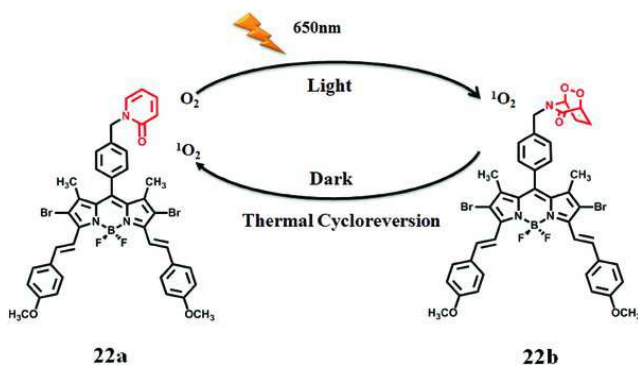

Figure 35. The cycle diagram of continuous release of $^1O_2$ based on bifunctional BODIPY derivative PS. Adapted from with permission.[94]
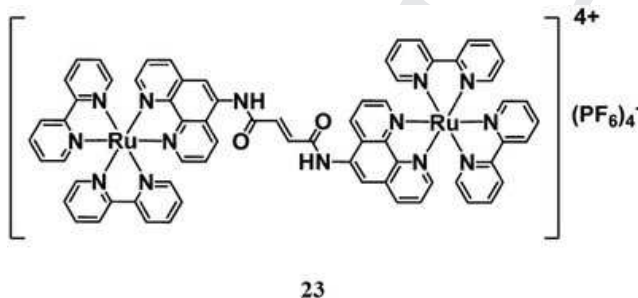

Figure 36. The structure of the binuclear ruthenium(II) dimer. Reproduced with permission.[95] Copyright 2014, The Royal Society of Chemistry.

previous $^1O_2$ quenching effect. With the further development of photochemistry and photophysics, these methods could also built up their own mechanisms in the future.

7. Conclusions and Outlook

In this review, we have summarized the recent developments in controllable photodynamic therapy and some novel strategies of designing activatable PSs. We introduced various regulation methods to control the $^1O_2$ production, such as PET, FRET, ICT, etc. These mechanisms can be employed to modulate the generation of $^1O_2$. It should be noted that the crucial concept of controllable PDT reagents is to selectively generate $^1O_2$ in tumor tissues and to avoid damaging normal tissues and organs. Based on PET mechanism, supramolecular photonic therapeutic reagents, environment-sensitive PSs and BODIPY derivatives have been reported, achieving $^1O_2$ on/off by pH or polarity variation. Amino protonation is the most used strategy to regulate PET process, and it is necessary to develop new method for effective PET switch. Controlling of FRET is one of the most common mechanism to modulate $^1O_2$ production. The key part of inhibitive FRET is to find a suitable linker, which can be cleaved by tumor-associated specific conditions such as lower pH and overexpression proteins or enzymes. Except for a cleaveable linker, using nano materials as carrier, combining PS and quencher into a single form is also effective to achieve switching of $^1O_2$ production. By regulating the energy level of FRET-acceptor, the direction of FRET can be inverted, resulting in an activation and deactivation of PS, respectively. Reversible FRET is becoming a promising strategy to modulate PDT. In addition, the using of photoconversion molecules and molecular logic-gates is also promising. In a word, by efficient FRET to quench PS, by prohibitive FRET to reactivate PS. Upon competing with ISC directly, ICT can effectively restrain the generation of $^1O_2$. The charge-transfer (CT) state of donor and acceptor can be influenced by solvent polarity and pH. However, ICT was rarely used to modulate PDT. There is still much room to apply ICT in activatable PDT.

Except for using various energy and electron transfer mechanism, physical confinement and controllable release of PS is also an important way to regulate PDT. As for this strategy, PS are always coated by some tumor targetable materials such as LDH or micelles, which can be decomposed only in tumor. In addition, the materials act as carrier and provide platform for incorporating many other functional molecules, achieving multiple treatment (such as photothermal therapy) and diagnose.

Tumor hypoxia and PDT-induced hypoxia seriously hinder the development of PDT. Therefore it is necessary to complement oxygen timely. Fortunately, $^1O_2$ can also be generated in dark due to the thermal conversion of endoperoxide, that is 'chemical control for $^1O_2$ release and capture'. We believed this strategy is promising.

Compared with traditional PDT reagents, which are untargetable, controllable PSs opens new avenue for PDT in clinical practice by selective control of photosensitization. However, some conditions required for controllable PDT have surpassed the normal physiological condition and some strategies are complicated or intricate. In addition, sometimes controllable PDT and high $^1O_2$ quantum yield cannot be achived simultaneously. Hence, it should be realized that even more wonderful strategies or PS should be designed to achieve more efficient and safer PDT.

ADVANCED
SCIENCE NEWS

www.advancedsciencenews.com

Author Proof

ADVANCED
SCIENCE
Open Access

www.advancedscience.com

Acknowledgements

Conflict of Interest

The authors declare no conflict of interest.

Keywords

[1] a) J. P. Celli, B. Q. Spring, I. Rizvi, C. L. Evans, K. S. Samkoe, S. Verma, B. W. Pogue, T. Hasan, *Chem. Rev.* **2010**, *110*, 2795; b) A. Kamkaew, S. H. Lim, H. B. Lee, L. V. Kiew, L. Y. Chung, K. Burgess, *Chem. Soc. Rev.* **2013**, *42*, 77; c) R. Liang, R. Tian, L. Ma, L. Zhang, Y. Hu, J. Wang, M. Wei, D. Yan, D. G. Evans, X. Duan, *Adv. Funct. Mater.* **2014**, *24*, 3144; d) T. Yogo, Y. Urano, Y. Ishitsuka, F. Maniwa, T. Nagano, *J. Am. Chem. Soc.* **2005**, *127*, 12162.

[2] a) L. Brannon-Peppas, J. O. Blanchette, *Adv. Drug. Deliver. Rev.* **2012**, *64*, 206; b) H. Fan, G. Yan, Z. Zhao, X. Hu, W. Zhang, H. Liu, X. Fu, T. Fu, X. B. Zhang, W. Tan, *Angew. Chem. Int. Ed.* **2016**, *55*, 5477; c) H. Gong, Z. Dong, Y. Liu, S. Yin, L. Cheng, W. Xi, J. Xiang, K. Liu, Y. Li, Z. Liu, *Adv. Funct. Mater.* **2014**, *24*, 6492; d) D. Chen, R. Tao, K. Tao, B. Chen, S. K. Choi, Q. Tian, Y. Xu, G. Zhou, K. Sun, *Small* **2017**, *13*, 1602053; e) H. Ren, J. Liu, F. Su, S. Ge, A. Yuan, W. Dai, J. Wu, Y. Hu, *ACS Appl. Mater. Interfaces* **2017**, *9*, 3463; f) H. Fan, G. Yan, Z. Zhao, X. Hu, W. Zhang, H. Liu, X. Fu, T. Fu, X. B. Zhang, W. Tan, *Angew. Chem. Int. Ed.* **2016**, *55*, 5477.

[3] a) P. Agostinis, K. Berg, K. A. Cengel, T. H. Foster, A. W. Girotti, S. O. Gollnick, S. M. Hahn, M. R. Hamblin, A. Juzeniene, D. Kessel, *Ca-Cancer J. Clin.* **2011**, *61*, 250; b) P. R. Ogilby, *Chem. Soc. Rev.* **2010**, *39*, 3181; c) M. J. Davies, *Biochem. Biophys. Res. Commun.* **2003**, *305*, 761; d) Y. Cakmak, S. Kolemen, S. Duman, Y. Dede, Y. Dolen, B. Kilic, Z. Kostereli, L. T. Yildirim, A. L. Dogan, D. Guc, *Angew. Chem.* **2011**, *123*, 12143.

[4] a) V. Bogoeva, M. Siksjo, K. G. Saeterbo, T. B. Melo, A. Bjorkoy, M. Lindgren, O. A. Gederaas, *Photodiagnosis Photodyn. Ther.* **2016**, *14*, 9; b) L. Zhou, S. Wei, X. Ge, J. Zhou, B. Yu, J. Shen, *J. Phys. Chem. B* **2012**, *116*, 12744. c) W. Wu, Y. Geng, W. Fan, Z. Li, L. Zhan, X. Wu, J. Zheng, J. Zhao, M. Wu, *RSC Adv.* **2014**, *4*, 51349.

[5] a) N. J. Turro, V. Ramamurthy, J. C. Scaiano, *Principles of molecular photochemistry: an introduction*, University Science Books, Sausalito, California, USA **2009**; b) E. I. Carrera, A. E. Lanterna, A. J. Lough, J.

C. Scaiano, D. S. Seferos, *J. Am. Chem. Soc.* **2016**, *138*, 2678; c) Y. P. Rey, D. G. Abradelo, N. Santschi, C. A. Strassert, R. Gilmour, *Eur. J. Org. Chem.* **2017**, https://doi.org/10.1002/ejoc.201601372; d) W. Wu, X. Wu, J. Zhao, M. Wu, *J. Mater. Chem. C* **2014**, *3*, 2291.

[6] a) N. Adarsh, R. R. Avirah, D. Ramaiah, *Org. Lett.* **2010**, *12*, 5720; b) S. G. Awuah, J. Polreis, V. Biradar, Y. You, *Org. Lett.* **2011**, *13*, 3884.

[7] J. Zhao, W. Wu, J. Sun, S. Guo, *Chem. Soc. Rev.* **2013**, *42*, 5323.

[8] a) Y. Liu, Y. Liu, W. Bu, C. Cheng, C. Zuo, Q. Xiao, Y. Sun, D. Ni, C. Zhang, J. Liu, *Angew. Chem. Int. Ed.* **2015**, *54*, 8105; b) S. Wang, H. Liu, J. Mack, J. Tian, B. Zou, H. Lu, Z. Li, J. Jiang, Z. Shen, *Chem. Commun.* **2015**, *51*, 13389; c) X. Zheng, X. Wang, H. Mao, W. Wu, B. Liu, X. Jiang, *Nat. Commun.* **2015**, *6*, 5834.

[9] a) K. Plaetzer, B. Krammer, J. Berlanda, F. Berr, T. Kiesslich, *Lasers Med. Sci.* **2009**, *24*, 259; b) G. Mazzone, A. D. Quartarolo, N. Russo, *Dyes and Pigments* **2016**, *130*, 9.

[10] a) A. E. O'Connor, W. M. Gallagher, A. T. Byrne, *Photochem. Photobiol.* **2009**, *85*, 1053; b) I.-W. Kim, J. M. Park, Y. J. Roh, J. H. Kim, M.-G. Choi, T. Hasan, *J. Photochem. Photobiol. B* **2016**, *159*, 14; c) X. Tan, X. Pang, M. Lei, M. Ma, F. Guo, J. Wang, M. Yu, F. Tan, N. Li, *Int. J. Pharm.* **2016**, *503*, 220.

[11] P. B. van Driel, M. C. Boonstra, M. D. Slooter, R. Heukers, M. A. Stammes, T. J. Snoeks, H. S. de Bruijn, P. J. van Diest, A. L. Vahrmeijer, P. M. v. B. en Henegouwen, *J. Control. Release* **2016**, *229*, 93.

[12] J. Eichler, J. Knof, H. Lenz, *Radiat. Environ. Biophys.* **1977**, *14*, 239.

[13] a) J. Zhao, S. Ji, W. Wu, W. Wu, H. Guo, J. Sun, H. Sun, Y. Liu, Q. Li, L. Huang, *RSC Adv.* **2012**, *2*, 1712; b) Y. You, W. Nam, *Chem. Soc. Rev.* **2012**, *41*, 7061; c) J. I. Goldsmith, W. R. Hudson, M. S. Lowry, T. H. Anderson, S. Bernhard, *J. Am. Chem. Soc.* **2005**, *127*, 7502.

[14] a) J. F. Lovell, T. W. Liu, J. Chen, G. Zheng, *Chem. Rev.* **2010**, *110*, 2839; b) J. Mou, P. Li, C. Liu, H. Xu, L. Song, J. Wang, K. Zhang, Y. Chen, J. Shi, H. Chen, *Small* **2015**, *11*, 2275; c) Z. Zha, X. Yue, Q. Ren, Z. Dai, *Adv. Mater.* **2013**, *25*, 777; d) Z. Peng, J. Qin, B. Li, K. Ye, Y. Zhang, X. Yang, F. Yuan, L. Huang, J. Hu, X. Lu, *Nanoscale* **2015**, *7*, 7682.

[15] a) X.-F. Zhang, W. Guo, *J. Photochem. Photobiol. A* **2011**, *225*, 117; b) I. Bruseghini, L. Fabbrizzi, M. Licchelli, A. Taglietti, *Chem. Commun.* **2002**, *13*, 1348.

[16] J. Fan, M. Hu, P. Zhan, X. Peng, *Chem. Soc. Rev.* **2013**, *42*, 29.

[17] Y. Urano, D. Asanuma, Y. Hama, Y. Koyama, T. Barrett, M. Kamiya, T. Nagano, T. Watanabe, A. Hasegawa, P. L. Choyke, *Nat. Med.* **2009**, *15*, 104.

[18] M. Abbas, Q. Zou, S. Li, X. Yan *Adv. Mater.* **2017**, *29*, 1605021.

[19] a) T. Miura, Y. Urano, K. Tanaka, T. Nagano, K. Ohkubo, S. Fukuzumi, *J. Am. Chem. Soc.* **2003**, *125*, 8666; b) Y. Urano, M. Kamiya, K. Kanda, T. Ueno, K. Hirose, T. Nagano, *J. Am. Chem. Soc.* **2005**, *127*, 4888; c) X. Wu, W. Wu, X. Cui, J. Zhao, M. Wu, *J. Mater. Chem. C* **2015**, *4*, 2843.

[20] X.-F. Zhang, *J. Fluoresc.* **2011**, *21*, 1559.

[21] a) M. E. Daraio, P. F. Aramendía, E. San Román, *Chem. Phys. Lett.* **1996**, *250*, 203; b) M. E. Daraio, A. Völker, P. F. Aramendía, E. San Román, *Langmuir* **1996**, *12*, 2932; c) R. Wang, Y. Geng, L. Zhang, W. Wu, W. Fan, Z. Li, L. Wang, L. Zhan, X. Wu, M. Wu, *Chin. J. Chem.* **2015**, *33*, 1251.

[22] a) K. Velmurugan, S. Suresh, S. Santhoshkumar, M. Saranya, R. Nandhakumar, *Luminescence* **2016**, *31*, 722; b) O. A. Bozdemir, R. Guliyev, O. Buyukcakir, S. Selcuk, S. Kolemen, G. Gulseren, T. Nalbantoglu, H. Boyaci, E. U. Akkaya, *J. Am. Chem. Soc.* **2010**, *132*, 8029; c) X. J. Jiang, P. C. Lo, S. L. Yeung, W. P. Fong, D. K. Ng, *Chem. Commun.* **2010**, *46*, 3188; d) S. Chakravarty, P. Dutta, S. Kalita, N. S. Sarma, *Sensors Actuat. B-Chem.* **2016**, *232*, 243; e) A. P. De Silva, H. N. Gunaratne, T. Gunnlaugsson, A. J. Huxley, C. P. McCoy, J. T. Rademacher, T. E. Rice, *Chem. Rev.* **1997**, *97*, 1515.

Q16

ADVANCED SCIENCE NEWS

www.advancedsciencenews.com

Author Proof

ADVANCED SCIENCE
Open Access

www.advancedscience.com

[23] S. O. McDonnell, M. J. Hall, L. T. Allen, A. Byrne, W. M. Gallagher, D. F. O'Shea, *J. Am. Chem. Soc.* **2005**, *127*, 16360.

[24] T. Yogo, Y. Urano, A. Mizushima, H. Sunahara, T. Inoue, K. Hirose, M. Iino, K. Kikuchi, T. Nagano, *Proc. Natl. Acad. Sci. USA* **2008**, *105*, 28.

[25] T. Inoue, K. Kikuchi, K. Hirose, M. Iino, T. Nagano, *Biorg. Med. Chem. Lett.* **1999**, *9*, 1697.

[26] W. Nakanishi, K. Kikuchi, T. Inoue, K. Hirose, M. Iino, T. Nagano, *Biorg. Med. Chem. Lett.* **2002**, *12*, 911.

[27] a) Ł. Lamch, W. Tylus, M. Jewgiński, R. Latajka, K. A. Wilk, *J. Phys. Chem. B* **2016**, *120*, 12768; b) M. Aliosman, M. Göksel, V. Mantareva, I. Stoineva, M. Durmuş, *J. Photochem. Photobiol. A* **2017**, *334*, 101; c) L. Dai, Y. Yu, Z. Luo, M. Li, W. Chen, X. Shen, F. Chen, Q. Sun, Q. Zhang, H. Gu, *Biomaterials* **2016**, *104*, 1.

[28] S. Ozlem, E. U. Akkaya, *J. Am. Chem. Soc.* **2008**, *131*, 48.

[29] U. Pischel, *Angew. Chem. Int. Ed.* **2007**, *46*, 4026.

[30] P. Montcourrier, P. Mangeat, C. Valembois, G. Salazar, A. Sahuquet, C. Duperray, H. Rochefort, *J. Cell Sci.* **1994**, *107*, 2381.

[31] I. Cameron, N. Smith, T. Pool, R. Sparks, *Cancer Res.* **1980**, *40*, 1493.

[32] L. Huang, J. Zhao, *J. Mater. Chem. C* **2015**, *3*, 538.

[33] J. Szöllosi, S. Damjanovich, L. Mátyus, *Cytometry* **1998**, *34*, 159.

[34] R. B. Sekar, A. Periasamy, *J. Cell Biol.* **2003**, *160*, 629.

[35] E.-Y. Chuang, C.-C. Lin, K.-J. Chen, D.-H. Wan, K.-J. Lin, Y.-C. Ho, P.-Y. Lin, H.-W. Sung, *Biomaterials* **2016**, *93*, 48.

[36] J. C. Qin, J. Yan, B. d. Wang, Z. y. Yang, *Tetrahedron Lett.* **2016**, *57*, 1935.

[37] V. Miskolci, B. Wu, Y. Moshfegh, D. Cox, L. Hodgson, *J. Immunol.* **2016**, *196*, 3479.

[38] a) M. Kotresh, K. Adarsh, M. Shivkumar, B. Mulimani, M. Savadatti, S. Inamdar, *Luminescence* **2015**, *31*, 760; b) L. Chang, X. W. He, L. Chen, Y. Zhang, *Nanoscale* **2017**, https://doi.org/10.1039/C6NR09944K; c) M. Ganiga, J. Cyriac, *Anal. Bioanal. Chem.* **2016**, *408*, 3699.

[39] Z. Bai, Y. Liu, P. Zhang, J. Guo, Y. Ma, X. Yun, X. Zhao, R. Zhong, F. Zhang, *Luminesc.* **2015**, *31*, 688.

[40] D. L. Dexter, *J. Chem. Phys.* **1953**, *21*, 836.

[41] C. G. Dos Remedios, P. D. Moens, *J. Struct. Biol.* **1995**, *115*, 175.

[42] J. F. Lovell, J. Chen, M. T. Jarvi, W. G. Cao, A. D. Allen, Y. Liu, T. T. Tidwell, B. C. Wilson, G. Zheng, *J. Phys. Chem. B* **2015**, *113*, 3203.

[43] a) N. S. James, P. Joshi, T. Y. Ohulchanskyy, Y. Chen, W. Tabaczynski, F. Durrani, M. Shibata, R. K. Pandey, *Eur. J. Med. Chem.* **2016**, *122*, 770; b) M. Bio, P. Rajaputra, Y. You, *Bioorg. Med. Chem. Lett.* **2016**, *26*, 145; c) R. Timor, H. Weitman, N. Waiskopf, U. Banin, B. Ehrenberg, *ACS Appl. Mater. Interfaces* **2015**, *7*, 21107; d) S. Haupt, I. Lazar, H. Weitman, M. O. Senge, B. Ehrenberg, *Phys. Chem. Chem. Phys.* **2015**, *17*, 11412.

[44] a) P. C. Ray, Z. Fan, R. A. Crouch, S. S. Sinha, A. Pramanik, *Chem. Soc. Rev.* **2014**, *43*, 6370; b) S. L. Robia, *J. Phys. Chem. B* **2015**, *119*, 1407; c) P. Ghenuche, M. Mivelle, T. J. De, S. B. Moparthi, H. Rigneault, N. F. Van Hulst, M. F. García-Parajó, J. Wenger, *Nano Lett.* **2015**, *15*, 6193; d) J. Saha, D. Dey, A. D. Roy, D. Bhattacharjee, S. A. Hussain, *J. Lumin.* **2016**, *172*, 168.

[45] a) M. Verhille, H. Benachour, A. Ibrahim, M. Achard, P. Arnoux, M. Barberi-Heyob, J.-C. Andre, X. Allonas, F. Baros, R. Vanderesse, *Curr. Med. Chem.* **2012**, *19*, 5580; b) T. Liu, M. Akens, J. Chen, B. Wilson, G. Zheng, *Photochem. Photobiol. Sci.* **2016**, *15*, 375; c) A. M. Bugaj, *Photochem. Photobiol. Sci.* **2011**, *10*, 1097; d) D. Wu, G. Song, Z. Li, T. Zhang, W. Wei, M. Chen, X. He, N. Ma, *Chem. Sci.* **2015**, *6*, 3839; e) T. W. Liu, J. Chen, G. Zheng, *Amino Acids* **2011**, *41*, 1123; f) T. W. Liu, M. K. Akens, J. Chen, B. C. Wilson, G. Zheng, *Photochem. Photobiol. Sci.* **2016**, *15*, 375; g) Y. Wei, C. Lu, Q. Chen, D. Xing, *Invest. Ophthalmol. Vis. Sci.* **2016**, *57*, 6011.

[46] J. Chen, K. Stefflova, M. J. Niedre, B. C. Wilson, B. Chance, J. D. Glickson, G. Zheng, *J. Am. Chem. Soc.* **2004**, *126*, 11450.

[47] M. Zhang, Z. Zhang, D. Blessington, H. Li, T. M. Busch, V. Madrak, J. Miles, B. Chance, J. D. Glickson, G. Zheng, *Bioconjug. Chem.* **2003**, *14*, 709.

[48] G. Zheng, J. Chen, K. Stefflova, M. Jarvi, H. Li, B. C. Wilson, *Proc. Natl. Acad. Sci. USA* **2007**, *104*, 8989.

[49] P.-C. Lo, J. Chen, K. Stefflova, M. S. Warren, R. Navab, B. Bandarchi, S. Mullins, M. Tsao, J. D. Cheng, G. Zheng, *J. Med. Chem.* **2008**, *52*, 358.

[50] a) R. Kalluri, M. Zeisberg, *Nat. Rev. Cancer* **2006**, *6*, 392; b) J. Lee, M. Fassnacht, S. Nair, D. Boczkowski, E. Gilboa, *Cancer Res.* **2005**, *65*, 11156; c) F. Cai, Z. Li, C. Wang, S. Xian, G. Xu, F. Peng, Y. Wei, Y. Lu, *BMB Rep.* **2013**, *46*, 252.

[51] E. Cló, J. W. Snyder, N. V. Voigt, P. R. Ogilby, K. V. Gothelf, *J. Am. Chem. Soc.* **2006**, *128*, 4200.

[52] K. V. Gothelf, A. Thomsen, M. Nielsen, E. Cló, R. S. Brown, *J. Am. Chem. Soc.* **2004**, *126*, 1044.

[53] H. Chen, J. Tian, W. He, Z. Guo, *J. Am. Chem. Soc.* **2015**, *137*, 1539.

[54] a) Y. Cho, H. Kim, Y. Choi, *Chem. Commun.* **2013**, *49*, 1202; b) L. Zhou, H. Jiang, S. Wei, X. Ge, J. Zhou, J. Shen, *Carbon* **2012**, *50*, 5594.

[55] F. Li, S. J. Park, D. Ling, W. Park, J. Y. Han, K. Na, K. Char, *J. Mater. Chem. B* **2013**, *1*, 1678.

[56] B. Tian, C. Wang, S. Zhang, L. Feng, Z. Liu, *ACS Nano* **2011**, *5*, 7000.

[57] J. Xu, F. Zeng, H. Wu, C. Yu, S. Wu, *ACS Appl. Mater. Interfaces* **2015**, *7*, 9287.

[58] L. Liu, L. Fu, T. Jing, Z. Ruan, L. Yan, *ACS Appl. Mater. Interfaces* **2016**, *8*, 8980.

[59] a) Y. Chen, P. Xu, Z. Shu, M. Wu, L. Wang, S. Zhang, Y. Zheng, H. Chen, J. Wang, Y. Li, *Adv. Funct. Mater.* **2014**, *24*, 4386; b) N. Ž. Knežević, V. Stojanovic, A. Chaix, E. Bouffard, K. E. Cheikh, A. Morère, M. Maynadier, G. Lemercier, M. Garcia, M. Garybobo, *J. Mater. Chem. B* **2016**, *4*, 1337; c) J. Wu, Y. Zhou, S. Li, D. Qu, W. H. Zhu, H. Tian, *Biomaterials* **2017**, *120*, 1; d) H. K. Yang, M. Qi, L. Mo, R. M. Yang, X. D. Xu, J. F. Bao, W. J. Tang, J. T. Lin, L. M. Zhang, X. Q. Jiang, *RSC Adv.* **2016**, *6*, 114519; e) H. Yan, L. Zhao, W. Shang, Z. Liu, W. Xie, C. Qiang, Z. Xiong, R. Zhang, B. Li, X. Sun, *Nano Res.* **2017**, *10*, 704.

[60] J. Zhao, L. Huang, X. Cui, S. Li, H. Wu, *J. Mater. Chem. B* **2015**, *3*, 9194.

[61] a) Z. Yang, J. H. Lee, H. M. Jeon, J. H. Han, N. Park, Y. He, H. Lee, K. S. Hong, C. Kang, J. S. Kim, *J. Am. Chem. Soc.* **2013**, *135*, 11657; b) X. Wu, X. Sun, Z. Guo, J. Tang, Y. Shen, T. D. James, H. Tian, W. Zhu, *J. Am. Chem. Soc.* **2014**, *136*, 3579; c) X. Chen, Y. Zhou, X. Peng, J. Yoon, *Chem. Soc. Rev.* **2010**, *39*, 2120.

[62] J. Han, W. Park, S. J. Park, K. Na, *ACS Appl. Mater. Interfaces* **2016**, *8*, 7739.

[63] S. Erbas-Cakmak, O. A. Bozdemir, Y. Cakmak, E. U. Akkaya, *Chem. Sci.* **2013**, *4*, 858.

[64] a) O. AltanáBozdemir, *Chem. Sci.* **2013**, *4*, 858; b) X. Mei, J. Wang, Z. Zhou, S. Wu, L. Huang, Z. Lin, Q. Ling, *J. Mater. Chem. C* **2017**, https://doi.org/10.1039/C6TC05519B.

[65] a) L. Zhang, A. M. Bluhm, K. J. Chen, N. E. Larkey, S. M. Burrows, *Nanoscale* **2017**, *9*, 1709; b) H. H. Deng, F. F. Wang, Y. H. Liu, H. P. Peng, K. L. Li, A. L. Liu, X. H. Xia, W. Chen, *J. Mater. Chem. C* **2016**, *4*, 7141; c) J.-c. Qin, Z.-y. Yang, *J. Photochem. Photobiol. A* **2016**, *324*, 152.

[66] a) J.-c. Qin, Z.-y. Yang, *J. Photochem. Photobiol. A* **2016**, *324*, 152; b) Y. Pan, Y. Shi, Z. Chen, J. Chen, M. Hou, Z. Chen, C.-W. Li, C. Yi, *ACS Appl. Mater. Interfaces* **2016**, *8*, 9472; c) B. Naskar, R. Modak, Y. Sikdar, D. K. Maiti, A. Banik, T. K. Dangar, S. Mukhopadhyay, D. Mandal, S. Goswami, *J. Photochem. Photobiol. A* **2016**, *321*, 99.

[67] L. Huang, W. Yang, J. Zhao, *J. Org. Chem.* **2014**, *79*, 10240.

[68] a) S. O. McDonnell, M. J. Hall, L. T. Allen, A. Byrne, W. M. Gallagher, D. F. O'Shea, *J. Am. Chem. Soc.* **2005**, *127*, 16360; b) T. Tørring,

ADVANCED SCIENCE NEWS

www.advancedsciencenews.com

Author Proof

ADVANCED SCIENCE
Open Access

www.advancedscience.com

R. Toftegaard, J. Arnbjerg, P. R. Ogilby, K. V. Gothelf, *Angew. Chem. Int. Ed.* **2010**, *49*, 7923.

[69] a) O. Nevskyi, D. Sysoiev, A. Oppermann, T. Huhn, D. Wöll, *Angew. Chem. Int. Ed.* **2016**, *55*, 12698; b) E. Hatano, M. Morimoto, K. Hyodo, N. Yasuda, S. Yokojima, S. Nakamura, K. Uchida, *Chem-Eur. J.* **2016**, *22*, 12680; c) S. Nishizawa, J. Hasegawa, K. Matsuda, *J. Phys. Chem. C* **2015**, *119*, 5117; d) D. Frath, T. Sakano, Y. Imaizumi, S. Yokoyama, T. Hirose, K. Matsuda, *Chemistry* **2015**, *21*, 11350; e) S. Bonacchi, M. ElGarah, A. Ciesielski, M. Herder, S. Conti, M. Cecchini, S. Hecht, P. Samorì, *Angew. Chem. Int. Ed.* **2015**, *54*, 4865; f) R. Kodama, K. Sumaru, K. Morishita, T. Kanamori, K. Hyodo, T. Kamitanaka, M. Morimoto, S. Yokojima, S. Nakamura, K. Uchida, *Chem. Commun.* **2014**, *51*, 1736; g) K. J. Chen, A. Charafeddin, B. Selvam, F. Boucher, A. D. Laurent, D. Jacquemin, *J. Phys. Chem. C* **2015**, *119*, 3684.

[70] L. Hou, X. Zhang, T. C. Pijper, W. R. Browne, B. L. Feringa, *J. Am. Chem. Soc.* **2014**, *136*, 910.

[71] J. Karolczak, D. Kowalska, A. Lukaszewicz, A. Maciejewski, R. P. Steer, *J. Phys. Chem. A* **2004**, *108*, 4570.

[72] C. Fan, S. Pu, G. Liu, *Dyes and Pigments* **2015**, *113*, 61.

[73] Y. Liu, G. Liu, X. Xu, Y. Chen, X. Wu, H. Wu, *Chem. Commun.* **2016**, *52*, 7966.

[74] J. Park, D. Feng, S. Yuan, H. C. Zhou, *Angew. Chem. Int. Ed.* **2015**, *54*, 430.

[75] J. Park, Q. Jiang, D. Feng, H. C. Zhou, *Angew. Chem. Int. Ed.* **2016**, *128*, 7304.

[76] a) S. S. Razi, R. Ali, R. C. Gupta, S. K. Dwivedi, G. Sharma, B. Koch, A. Misra, *J. Photochem. Photobiol. A* **2016**, *324*, 106; b) J. Wang, Y. Chen, C. Yang, T. Wei, Y. Han, M. Xia, *RSC Adv.* **2016**, *6*, 33031; c) Z. Lu, J. Wu, W. Liu, G. Zhang, P. Wang, *RSC Adv.* **2016**, *6*, 32046.

[77] a) Y. M. Zhang, W. J. Qu, G. Y. Gao, B. B. Shi, G. Y. Wu, T. B. Wei, Q. Lin, H. Yao, *New J. Chem.* **2014**, *38*, 5075; b) X. Huang, C. Fan, Z. Wang, X. Zhan, M. Pei, Z. Lu, *Inorg. Chem. Commun.* **2015**, *57*, 62; c) T. Wei, J. Wang, Y. Chen, Y. Han, *RSC Adv.* **2015**, *5*, 57141.

[78] a) Y. Miao, B. Zhao, Z. Gao, H. Shi, P. Tao, Y. Wu, K. Wang, H. Wang, B. Xu, F. Zhu, *Org. Electron.* **2017**, *42*, 1; b) C. H. Lim, M. D. Ryan, B. G. McCarthy, J. C. Theriot, S. M. Sartor, N. H. Damrauer, C. B. Musgrave, G. M. Miyake, *J. Am. Chem. Soc.* **2017**, *139*, 348; c) H. Naito, K. Nishino, Y. Morisaki, K. Tanaka, Y. Chujo, *Angew. Chem. Int. Ed.* **2017**, *56*, 254.

[79] a) L. Vachova, V. Novakova, K. Kopecky, M. Miletin, P. Zimcik, *Dalton Trans.* **2012**, *41*, 11651; b) V. Novakova, P. Hladik, T. Filandrova, I. Zajicova, V. Krepsova, M. Miletin, J. Lenco, P. Zimcik, *Phys. Chem. Chem. Phys.* **2014**, *16*, 5440; c) V. Novakova, P. Zimcik, M. Miletin, L. Vachova, K. Kopecky, K. Lang, P. Chabera, T. Polivka, *Phys. Chem. Chem. Phys.* **2010**, *12*, 2555; d) M. G. Ren, M. Mao, Q. H. Song, *Chem. Commun.* **2012**, *48*, 2970.

[80] X. F. Zhang, X. Yang, *J. Phys. Chem. B* **2013**, *117*, 9050.

[81] a) W. Pang, X. F. Zhang, J. Zhou, C. Yu, E. Hao, L. Jiao, *Chem. Commun.* **2012**, *48*, 5437; b) S. Duman, Y. Cakmak, S. Kolemen, E. U. Akkaya, Y. Dede, *J. Org. Chem.* **2012**, *77*, 4516.

[82] K. Hirakawa, Y. Nishimura, T. Arai, S. Okazaki, *J. Phys. Chem. B* **2013**, *117*, 13490.

[83] a) D. Margulies, C. E. Felder, G. Melman, A. Shanzer, *J. Am. Chem. Soc.* **2007**, *129*, 347; b) M. Semeraro, A. Credi, *J. Phys. Chem. C* **2010**, *114*, 3209; c) P. Remón, M. Bälter, S. Li, J. Andréasson, U. Pischel, *J. Am. Chem. Soc.* **2011**, *133*, 20742.

[84] S. Erbas-Cakmak, E. U. Akkaya, *Angew. Chem. Int. Ed.* **2013**, *52*, 11364.

[85] X. S. Li, M. R. Ke, W. Huang, C. H. Ye, J. D. Huang, *Chem-Eur. J.* **2015**, *21*, 3310.

[86] a) K. Ma, R. Xing, T. Jiao, G. Shen, C. Chen, J. Li, X. Yan, *ACS Appl. Mater. Interfaces* **2016**, *8*, 30759; b) N. Zhang, F. Zhao, Q. Zou, Y. Li, G. Ma, X. Yan, *Small* **2016**, *12*, 5936; c) R. Xing, T. Jiao, K. Ma, G. Ma, H. Mohwald, X. Yan, *Sci. Rep.* **2016**, *6*, 26506; d) Y. Yang, H. Liu, M. Han, B. Sun, J. Li, *Angew. Chem. Int. Ed.* **2016**, *55*, 13538.

[87] K. Liu, R. Xing, Q. Zou, G. Ma, H. Mohwald, X. Yan, *Angew. Chem. Int. Ed.* **2016**, *55*, 3036.

[88] J. Tan, C. Sun, K. Xu, C. Wang, J. Guo, *Small* **2015**, *11*, 6338.

[89] D. Ling, W. Park, S. J. Park, Y. Lu, K. S. Kim, M. J. Hackett, B. H. Kim, H. Yim, Y. S. Jeon, K. Na, T. Hyeon, *J. Am. Chem. Soc.* **2014**, *136*, 5647.

[90] a) N. J. Turro, F. C. Ming, *J. Am. Chem. Soc.* **1981**, *103*, 7218; b) J. M. Aubry, C. Pierlot, J. Rigaudy, R. Schmidt, *Acc. Chem. Res.* **2003**, *36*, 668.

[91] J. Xu, S. Sun, Q. Li, Y. Yue, Y. Li, S. Shao, *Analyst* **2015**, *140*, 574.

[92] C. Robertson, D. H. Evans, H. Abrahamse, *J. Photochem. Photobiol. B* **2009**, *96*, 1.

[93] S. Kolemen, T. Ozdemir, D. Lee, G. M. Kim, T. Karatas, J. Yoon, E. U. Akkaya, *Angew. Chem. Int. Ed.* **2016**, *55*, 3606.

[94] I. S. Turan, A. Yildiz, A. Turksoy, G. Gunaydin, E. U. Akkaya, *Angew. Chem. Int. Ed.* **2016**, *55*, 2875.

[95] K. Lou, J. F. Lovell, *Chem. Commun.* **2014**, *50*, 3231.

1700113 (17 of 17)

Q1   APT to AU: Please confirm that copyright permissions for reproduction of all figures have been obtained and all copyright lines are correct. Please note that for all Wiley journals the line: 'Copyright Year, Wiley ...' can be omitted, though the permission is still required.

Q2   APT to AU: Please confirm that figure 1 is wholly original, has not been published elsewhere, and no copyright permission is required.

Q3   APT to AU: Please confirm that figure 2 is wholly original, has not been published elsewhere, and no copyright permission is required.

Q4   **APT to AU: In most figures (all figures except for 1-3, 9, 13-15, 18, 21, 23, 24, 26, and 31) bold numbers for chemical compounds are present. These numbers do not seem to refer to any numbers within your manuscript. Please check and possibly provide corrected figures.**

Q5   APT to AU: Unfortunately, the number of biographies we can publish is limited to three. We removed Dr. Wu's biography, accordingly. Please let us know if this is correct.

Q6   APT to AU: Please confirm that figure 7 is wholly original, has not been published elsewhere, and no copyright permission is required. Please note that Figure 8 seems to be missing in production data. Please provide this figure and corresponding figure caption.

Q7   APT to AU: Please note that Figure 8 seems to be missing in production data. Please provide this figure and corresponding figure caption.

Q8   APT to AU: Please confirm that figure 9 is wholly original, has not been published elsewhere, and no copyright permission is required.

Q9   APT to AU: Please confirm that figure 16 is wholly original, has not been published elsewhere, and no copyright permission is required.

Q10   APT to AU: Please confirm that figure 17 is wholly original, has not been published elsewhere, and no copyright permission is required.

Q11   APT to AU: Please confirm that figure 20 is wholly original, has not been published elsewhere, and no copyright permission is required.

Q12   APT to AU: Please confirm that figure 21 is wholly original, has not been published elsewhere, and no copyright permission is required.

Q13   APT to AU: Please confirm that figure 24 is wholly original, has not been published elsewhere, and no copyright permission is required.

Q14   APT to AU: Please confirm that figure 26 is wholly original, has not been published elsewhere, and no copyright permission is required.

Q15   APT to AU: Please confirm that figure 27 is wholly original, has not been published elsewhere, and no copyright permission is required.

Q16   APT to AU: Please provide volume and first page number or manuscript number for reference 5c if available now.

Q17   APT to AU: Please provide volume and first page number or manuscript number for reference 38b if available now.

Q18   APT to AU: Please provide volume and first page number or manuscript number for reference 64b if available now.